

**UNCLASSIFIED**

**AD 419043**

**DEFENSE DOCUMENTATION CENTER**

**FOR**

**SCIENTIFIC AND TECHNICAL INFORMATION**

**CAMERON STATION, ALEXANDRIA, VIRGINIA**



**UNCLASSIFIED**

NOTICE: When government or other drawings, specifications or other data are used for any purpose other than in connection with a definitely related government procurement operation, the U. S. Government thereby incurs no responsibility, nor any obligation whatsoever; and the fact that the Government may have formulated, furnished, or in any way supplied the said drawings, specifications, or other data is not to be regarded by implication or otherwise as in any manner licensing the holder or any other person or corporation, or conveying any rights or permission to manufacture, use or sell any patented invention that may in any way be related thereto.

64-5

5 731250

1

419043

ASTIA DIVISION 24

RESEARCH AND DEVELOPMENT

ON

PHOTO-CONDUCTIVE PHOTO-TAPE

FIRST INTERIM REPORT

September 1963

Air Force Systems Command  
Aeronautical Systems Division  
Wright-Patterson Air Force Base, Ohio

Project No. 6263, Task No. 626302

DDC  
OCT 8 1963  
TISIA B

(Prepared under Contract No. AF 33(657)-11485  
by the Astro-Electronics Division  
of Radio Corporation of America,  
Princeton, New Jersey.)

AD No. \_\_\_\_\_  
DDC FILE COPY

419043

B 7. 103

5

731250

ASTIA DIVISION 24

6 RESEARCH AND DEVELOPMENT

ON

PHOTO-CONDUCTIVE PHOTO-TAPE,

9  
FIRST INTERIM REPORT, no. 1  
11 September 1963,

Air Force Systems Command  
Aeronautical Systems Division  
Wright-Patterson Air Force Base, Ohio

AI

16 Project No. 6263, Task No. 626302  
17

(Prepared under Contract No. AF 33(657)-11485  
by the Astro-Electronics Division  
of Radio Corporation of America,  
Princeton, New Jersey.)

## FOREWORD

This report was prepared by the Astro-Electronics Division of the Radio Corporation of America, Princeton, N.J., Under Contract No. AF33(657)11485. This contract was initiated under Project No. 6263, "Electro-Optical Techniques for Reconnaissance," Task No. 626302, "Electro-Optical Sensing, Storage and Information Processing." This work was administered under the direction of the Directorate of the Air Force Avionics Laboratory, Research and Technology Division, Aeronautical Systems Division, with Mr. James P. Fulton acting as Project Engineer.

# TABLE OF CONTENTS

## CHAPTER I. INTRODUCTION

## CHAPTER II. APPLIED RESEARCH

Section	Page
I. PHOTO-TAPE RESEARCH .....	3
A. ELECTRON OPTICS	
1. Narrow Separation Characteristic .....	3
2. Beam Resolution Parameters .....	4
3. Permanent-Magnet Focus Assembly .....	6
B. CONTINUOUS TAPE MACHINE .....	7
1. Machine Modifications .....	7
2. Sensitivity of Tape Samples .....	7
C. BEARINGS .....	8
D. FLOOD GUNS .....	9
E. STORED-SIGNAL ENHANCEMENT BY SECONDARY EMISSION .....	9
1. Experimental Activity .....	9
2. Theoretical Possibilities .....	10
F. ELECTRON-BEAM SPOT SIZE .....	11
II. PHOTOCONDUCTOR RESEARCH .....	12
A. MODIFICATION OF TEST APPARATUS .....	12
B. EFFECTS OF REVERSED DIRECTION OF ILLUMINATION.....	12
C. PHOTOCONDUCTIVE GAIN OF "MIXED SELENIDES"....	14
III. ELECTRON-GUN RESEARCH .....	18
A. INTRODUCTION .....	18
B. CONVERGENT-FLOW PIERCE-TYPE GUN .....	18
C. OTHER GUN CONFIGURATIONS .....	19

TABLE OF CONTENTS (Continued)

Section	Page
1. Triode Gun with Modified Spacing .....	19
2. Gun with Smooth Metallic Cathode .....	19
3. Lanthanum-Hexaboride Cathode .....	20
4. Phillips Cathodes .....	20
 CHAPTER III. DEMONSTRATION MODEL CAMERAS 	
I. CAMERA I OPERATION AND COMPONENT TESTING	
A. OPTICAL TESTS ON CAMERA I .....	23
B. READ-GUN TESTS .....	28
II. CAMERA II SYSTEM ASSEMBLY .....	29
A. GENERAL .....	29
B. SYSTEM SPECIFICATIONS .....	29
C. CIRCUITRY .....	30
1. Video Preamplifier .....	30
2. Video Amplifier .....	30
3. Horizontal Deflection .....	33
4. Vertical Deflection .....	33
5. Control Circuitry .....	34
a. General Description .....	34
b. Flood-Gun Control .....	35
c. Read-Gun Control .....	35
6. Sync Generator .....	36
7. Exposure Control (Shutter Delay) .....	36
8. Shutter Drive .....	37
9. Alignment Coil Current Regulators .....	39
10. One-Frame Readout Circuit .....	39
11. System Interlock .....	39
12. Focus-Current Supply .....	43
D. ASSEMBLY LAYOUT .....	43
1. Video Amplifier and Deflection Assembly .....	43
2. Power Supply and Control Assembly .....	45
E. INTERFERENCE ANALYSIS .....	46
1. Jitter .....	46
2. Hum .....	50

TABLE OF CONTENTS (Continued)

Section	Page
III. SUBSYSTEM DEVELOPMENT .....	51
A. CAMERA III ENCLOSURE MODIFICATIONS.....	51
1. Negator Brake .....	51
2. Electrostatic Platens .....	52
3. Magnetic Plug .....	52
4. Tape Guides .....	54
5. Aperture Plate Brace .....	54
6. Planar Lens Mounting .....	54
7. Sensor Head Vacuum Problem .....	54
B. HIGH-RESOLUTION MONITOR .....	54
1. Mechanical Assembly .....	54
2. Circuitry .....	56
a. Video-Amplifier Circuit .....	56
b. Horizontal-Deflection Circuit .....	56
c. Vertical-Deflection Circuit .....	56
C. TEST CHART ILLUMINATOR .....	57
IV. OPTICS .....	58
V. ELECTRON BEAM FILM RECORDER SUPPORT .....	61
A. ELECTRON GUN .....	61
B. DEFLECTION YOKE .....	61
C. DYNAMIC FOCUS, CURRENT GENERATOR, AND AMPLIFIER .....	63
D. BEAM ALIGNMENT AND SHIELDING .....	63
E. FILM AND DEGASSING.....	63
F. MEASUREMENTS .....	63
G. BEARINGS .....	63



## LIST OF ILLUSTRATIONS

Figure		Page
1.	Separator Characteristic for Bent-Beam Monoscope Tube .....	4
2.	Resolution of Square-Wave Input at 50-percent Response as a Function of $B_t/B_g$ .....	5
3.	Resolution of Square-Wave Input at 50-percent Response as a Function of $V_{G_2}$ .....	5
4.	Resolution as a Function of Heater Current (emission density) .....	6
5.	Current-Voltage Characteristic for Gap-Cell No. 1 .....	16
6.	Spectral Response of Gap Cell and Standard Storage Target .....	17
7.	Variation of Response of Gap Cell with Light Intensity for Different Applied Fields .....	17
8.	Sine-Wave Response Curve of Film Type No. SO-132 at High Contrast .....	24
9.	Video Amplifier .....	31
10.	Video Amplifier Stages, View A and B .....	32
11.	Control Chassis .....	34
12.	Shutter-Drive Circuit, Schematic Diagram .....	38
13.	System Interlock .....	40
14.	System Interlock, Camera II, Schematic Diagram .....	41
15.	Scheme for Minimizing Ground Loops and Optimizing Magnetic Cancellation .....	45
16.	Saturation Curves for Two-Layer Material, Coated Outside Only .....	50
17.	Emergency Brake for Tape-Transport Mechanism .....	52
18.	Emergency Brake for Tape-Transport Mechanism, Orthographic Projection .....	53
19.	High-Resolution Monitor .....	55
20.	Test Chart Illuminator .....	57
21.	Transfer and Density Characteristic Curves for EBFR Gun No. 4 .....	62

## LIST OF TABLES

Table		Page
I.	Bearing Test Data, August 1963 .....	8
II.	Comparative Sensitivities of Selected Targets for Illumination from Opposite Directions .....	13
III.	Resolution Data for Photographs taken with the Minus-Red Filter .....	27
IV.	Extreme Value for Shutter Delays .....	37
V.	Specifications for Focus-Current Supply .....	44
VI.	Specifications for Extra Current Supply .....	44

## CHAPTER I. INTRODUCTION

This is the first interim engineering report on a program of Research and Development on Photoconductive Photo-Tape. It covers the effort of June through August 1963. The program is directed toward the development of techniques and demonstration equipment for a system to store optical images of electrostatic charges distributed on a tape.

This program is divided into two primary areas, the first of which is the demonstration of specified performance levels in terms of available hard-copy records out of the reproducer, using the laboratory models available. The second is to demonstrate the feasibility of building higher-performance cameras based on the Photo-Tape concept by employing laboratory models of individual components.

The performance levels, specified as Level A, Level B, and Level C, have been divided into three groups of parameters (Level A being the minimum and Level C the optimum) as defined in the governing work statement.

The effort on the Photo-Tape program has four objectives which, in chronological order of achievement are:

1. To demonstrate a frame camera at Level A,
2. To demonstrate the feasibility of a frame camera at Level B,
3. To demonstrate the performance of a frame camera at Level B, and, finally,
4. To carry out the necessary applied research effort to support the above goals and to show the feasibility of a frame camera at Level C at the earliest possible date.

Research is summarized concerning electron optics, photoconductors, electron guns, and development of demonstration model cameras.

## CHAPTER II. APPLIED RESEARCH

### SECTION I. PHOTO-TAPE RESEARCH

#### A. ELECTRON OPTICS

##### 1. Narrow Separation Characteristics

Tests made with the bent-beam monoscope tubes (using the electron gun configuration designed for redistributionless readout) showed that the velocity spread of the return beam of secondary electrons is affected by the alignment fields. The smallest velocity spread obtained produced the separator characteristic shown in Figure 1. This characteristic, which is much steeper than the characteristic shown in Figure 37 of the Final Report prepared under the previous contract\* is consistent with the integral of the secondary-electron-emission energy distribution.

The steeper slope of this separator characteristic indicates greater readout sensitivity than that provided by the previous characteristic, by a factor of about three. Careful measurement of the signal-to-noise ratio produced by a sine-wave modulation of the target potential yielded a measured ratio slightly less than that predicted by theory. The explanation for the discrepancy observed during work on the previous contract\* between the measured and the theoretical signal-to-noise ratio is that the broad characteristic had been included in the theoretical formulation. However, the actual separator characteristic during the signal-to-noise measurements was apparently narrow.

Additional measurements are required to determine why the velocity spread is so greatly affected by the alignment. A bent-beam monoscope tube that includes the first printed internal-alignment coil was made for this purpose. Unfortunately, the first printed coil has a high outgassing rate, and the 1-liter-per-second ion pump attached to the tube has not yet brought the pressure down far enough to permit testing. The pump is in continuous operation and the pressure may yet be reduced to a value that will permit tube operation. Precautions to reduce outgassing on the new alignment coils are being taken.

---

\*Contract No. AF 33(616)-6365 (Applied Research on Television Photo-Tape)

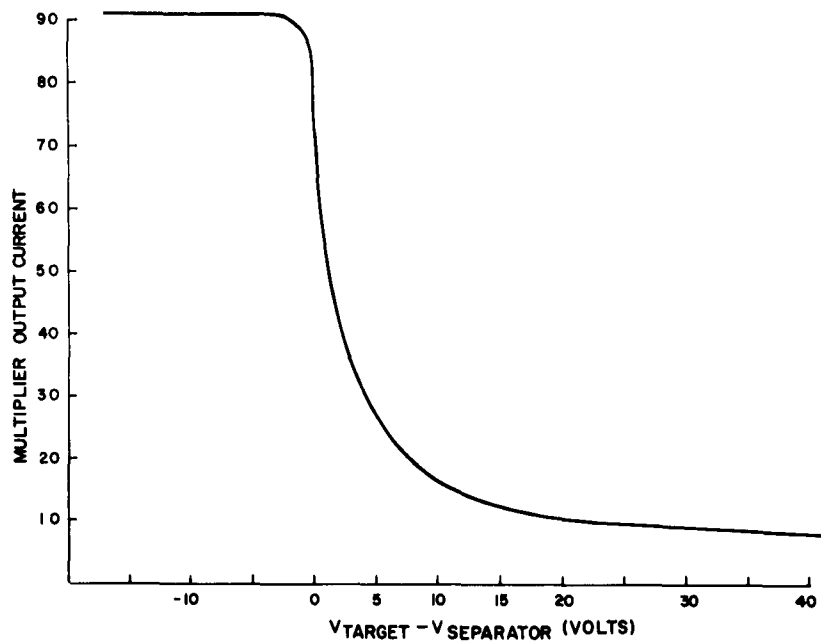


Figure 1. Separator Characteristic for Bent-Beam Monoscope Tube

## 2. Beam Resolution Parameters

A number of tests were made with a 3-inch monoscope tube to determine how the beam resolution varied with focusing parameters. When the target flux density,  $B_t$ , was held constant at each of three values, and the gun flux density,  $B_g$ , was varied, the resolution varied as shown in Figure 2. Note that the resolution does not improve significantly for a  $B_t$  greater than 150 gauss, or for a  $B_t/B_g$  greater than 8.

Apparently, demagnification of the beam spot by increasing the gradient of the magnetic field is effective in improving resolution until the aberration produced by the velocity spread overrides the benefits of demagnification. The resolution was affected very little by the flux density between gun and target (except that it decreased for abrupt changes in the field), but depended only on the end values.

Resolution was not a function of the  $G_2$  voltage when the control grid was changed correspondingly to maintain constant beam current as shown in Figure 3.

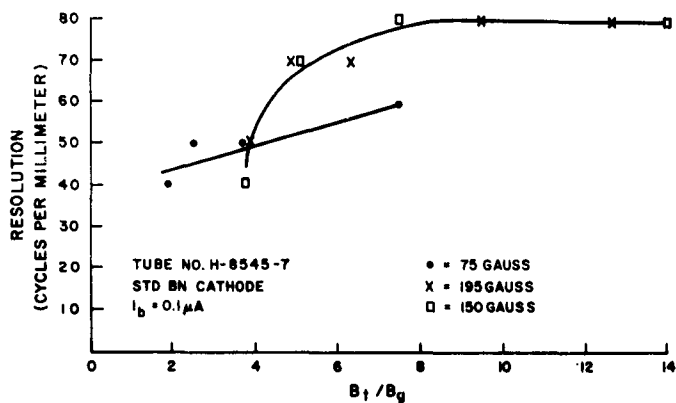


Figure 2. Resolution of Square-Wave Input at 50-percent Response as a Function of  $B_t/B_g$

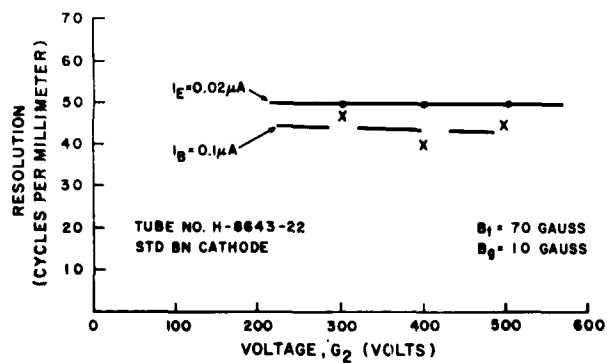


Figure 3. Resolution of Square-Wave Input at 50-percent Response as a Function of  $V_{G_2}$

The resolution was not a function of heater current (and consequently of emission density) for values above 0.575 ampere, as shown in Figure 4. Normal heating current is 0.65 ampere. These measurements were taken with  $B_t = 72$  gauss. Higher resolution was observed than in the data shown in Figure 3; the gun apparently improved with age.

A gun was made and tested in which the  $G_1$  cup and certain other parts were made of magnetic steel instead of the normal non-magnetic material. The resolution of this gun was the same as that of standard guns, even though the magnetic  $G_1$  could have caused as much as a 4-to-1 reduction of the focus field inside the  $G_1$ -K space. Either reducing the flux did not help, or the operating temperature of the  $G_1$  was too close to its Curie point ( $750^\circ\text{C}$ ).

### 3. Permanent-Magnet Focus Assembly

A number of ferrite ring magnets were obtained to be used in the design of a permanent-magnet focus assembly. An arrangement of rings was obtained that yielded the proper focus-field configuration. The results of this experiment indicate an adequate focus magnet can be made of alnico bars. The total weight would be comparable to that of a conventional focus coil.

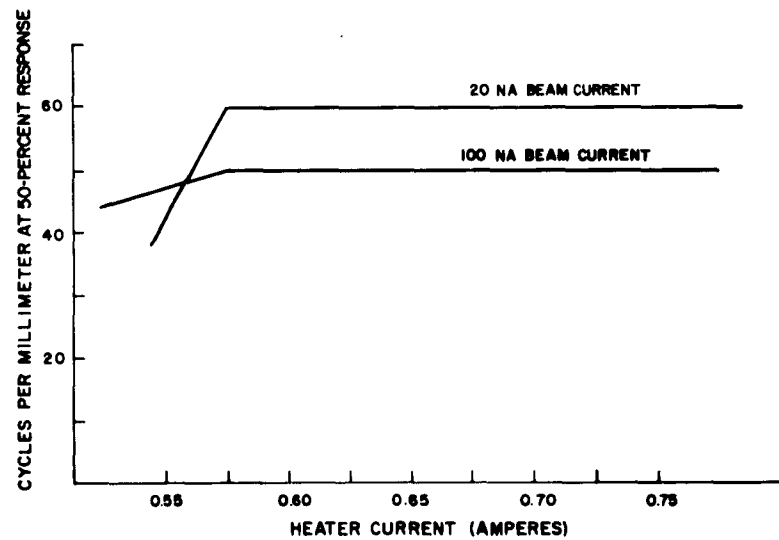


Figure 4. Resolution as a Function of Heater Current (Emission Density)

## B. CONTINUOUS TAPE MACHINE

### 1. Machine Modifications

The results of the work performed with the the tape machine during the past year indicate that a large number of modifications are required to improve the quality of the tape produced. However, until the present period, these modifications could not be introduced because of the continuous demand for tapes. Recently this demand has been alleviated and the vacuum chamber was sent to the Model Shop to be machined so as to accommodate the new components. The improved components, such as the tape drive, evaporators, and polystyrene applicator, are being designed or constructed.

The major advance being prepared is the provision for deposition of all films on the tape in a single evacuation of the chamber. Until now it has been necessary to open the chamber, remove the evaporators, and install the polystyrene applicator, before the polystyrene could be formed on the photoconductor. This improvement is expected to eliminate the imperfections in the tape caused by dust collected during this equipment change.

### 2. Sensitivity of Tape Samples

Sensitivity measurements obtained in Camera I for three tapes are tabulated below.

Tape No.	Material	Sensitivity (volts/foot-candle-second)
47	(As <sub>2</sub> Se <sub>3</sub> )	75
51	(As <sub>2</sub> Se <sub>3</sub> + Al barrier layer)	60
56	(mixed selenides)	38

Tape No. 56 was used for the last set of pictures taken with the Camera I Electron-Beam Film Recorder system. Demountable measurements of a sample of Tape No. 56 taken from an end of the tape indicated high sensitivity. Tape No. 47 was used in January for the measurements program; Tape No. 51 was inserted in the system briefly before Tape No. 56, but it was removed when cracks were discovered. Additional experiments are planned on the mixed-selenide tapes.

The optical absorption of target No. 10 (As<sub>2</sub>Se<sub>3</sub>) and of target No. 15 (Sb<sub>2</sub>S<sub>3</sub> + Sb) was measured on a Cary spectrophotometer. For each material, 50 percent of maximum absorption occurred at 0.7 to 0.72 micron. For Sb<sub>2</sub>Se<sub>3</sub>, 50 percent absorption occurred at 0.8 micron.



### C. BEARINGS

The most recent bearing-test data is presented in Table I. The irradiated BarTemp bearings are behaving like normal BarTemp bearings.

ITI\* has reported on the bearings that were returned for inspection. The irradiated bearings showed light-to-moderate race wear, and light deposits of MoS<sub>2</sub> on the balls and races. There was nothing in the report to explain the high friction previously observed.

TABLE I. BEARING TEST DATA, AUGUST 1963

Bearing Test	Average Speed	Total Time	Pressure Range	Remarks
BarTemp 9A	1210	12395	1	Irradiated  No MoS <sub>2</sub>
BarTemp 10	1075	9690	1	
BarTemp 21	615	2280	2	
BarTemp 22	450	3888	2	
BarTemp 23	325	3072	2	
BarTemp 19	800	2712	2	
Barden 30	500	7800	2	
Barden 31	450	4172	2	
Barden 32	550	3580	2	
ITI-1-4373-CBS	850	10782	1	
ITI-1-4380-TiC	1180	12160	1	

**NOTES:**

Pressure Range 1 is 10<sup>-6</sup> to 10<sup>-8</sup> torr.

Pressure Range 2 is 10<sup>-7</sup> to 10<sup>-8</sup> torr.

\*Industrial Techtronics, Inc.

#### **D. FLOOD GUNS**

A heavy deposit of polymerized pump oil was discovered on the window of the flood gun used in Camera I during the last measurements program. The window transmission was 50 percent, and the previously reported sensitivities should be increased accordingly.

The deposit was also observed on the back side of the shield. This indicates that the electrons may traverse an appreciable distance between the tape and the shield. If it were desired to store pictures close to one another along the tape it would be necessary to improve the shield design; otherwise the electrons from one exposure would erase information written during the previous exposure.

A new flood-gun was designed to deliver a larger fraction of the cathode current to the tape than the present gun in Camera I.

#### **E. STORED-SIGNAL ENHANCEMENT BY SECONDARY EMISSION**

##### **1. Experimental Activity**

Experiments were made with the process of amplifying the voltage pattern stored on an insulator by bombarding the insulator with electrons and collecting all of the secondary electrons that are generated. Stretching of the signal will occur if the secondary emission ratio depends on the target voltage. It is recognized at the start that the bombardment process is in itself noisy, so that the signal-to-noise ratio stored in the target is degraded. However, the possibility for improved signal-to-noise ratio for the entire system does exist.

A one-centimeter-square polystyrene target in a 3-inch image-orthicon bottle was used for these tests. Half of the target was made one-to-three volts negative with respect to the other half by scanning the first half for a short time with a low-velocity beam. The one-to-three volt pattern was enhanced by bombarding with electrons of about 50 volts energy.

The maximum slope of the secondary-emission-ratio curve for polystyrene occurs between 30 and 100 volts, with  $\delta = 1$  at about 50 volts. Thus, bombarding at about 50 volts produced the maximum enhancement with the smallest d-c voltage change for the whole target.

To date, the maximum increase in the stored voltage obtained has been a factor of two. The experiments have not progressed either to the point of determining why a gain of only two has been obtained, or to the point of providing conclusive support for the analysis presented in the next section.

## 2. Theoretical Possibilities

The enhancement process was analyzed to predict the signal-to-noise change produced by the electron bombardment. The analysis was not completely written in final form at the closing date of this report, but some informative numbers are available.

This starting data was used:

<u>Measured Values</u>	<u>Operating Parameters</u>
$(d\delta/dV)_t \text{ max}$	= 0.005 per volt 80 cy/mm
$C_i$	= 5.0 nf/cm <sup>2</sup> 2 to 1 contrast
Maximum readable signal	= 6 v p-p 0.5 v p-p written
	Tape x lens response = 0.5

where

$\delta$  is the secondary emission,

$V_t$  is the insulator surface voltage at the target, and

$C_i$  is the insulator capacitance.

The  $C_i$  chosen here corresponds to that of actual tapes, and is a higher capacitance target than that which was used as the basis for discussion of this effect with ASD personnel on August 19, 1963. This new choice leads to a more favorable prospect for signal-stretching.

The assignment of maximum readable signal corresponds to the narrow, more sensitive separator characteristic discussed earlier in this report. It is assumed that it will be possible to adjust the readout conditions so that the stretched background in the low-contrast picture will fall outside the dynamic range of readout.

The following results are obtained:

	Lens x Tape Response at 80 cy/mm	
	<u>100 percent</u>	<u>50 percent</u>
1. S/N, exposure alone	55.3	29.5
2. S/N, exposure plus enhancement	26.1	13.3
3. S/N, 20 na, exposure alone	8.3	2.2
4. S/N, 20 na beam, exposure plus enhancement	22.3	11.1
5. S/N, 200 na beam, exp. alone	24.0	7.1

If the lens and tape had 100-percent response at 80 cycles per millimeter, the S/N from the photon input in an area corresponding to 80-cycles-per-millimeter resolution would be 55.3. If the lens and tape had 50-percent response at 80 cycles per millimeter the corresponding S/N from the photon input would be 29.5. After enhancement, the S/N stored on the tape drops to the values given in line 2 above.

The stored signal read directly with a 20-nanoampere readout beam produces the S/N given in line 3. If the enhanced signal is read with a 20-nanoampere readout beam, the S/N is as given in line 4. Reading the stored signal directly with a 200-nanoampere beam produces the S/N value given in line 5.

It was assumed in these calculations that the enhancement process continued until the voltage pattern on the tape was large enough to produce the largest possible modulation of the return beam. Thus additional enhancement cannot provide any advantage. Note that an increase in beam-current density by a factor of ten provides about the same improvement as the maximum possible enhancement. Also, if the beam-current density were extremely high, the readout S/N could approach 26.1 (or 13.3) if enhancement were used, while it could approach 55.3 (or 28.5) if enhancement were not used.

#### F. ELECTRON-BEAM SPOT SIZE

An estimate for the spot size of an electron beam was derived for the case of the magnetic and electric fields in a redistributionless readout structure. It was formulated to give the diameter,  $d$ , of the spot formed by thermal electrons emitted with initial axial energy  $V_1$ , when conditions are such that axial electrons with initial energy  $V_2$  are focused to a point. The form of the equation is

$$d = \frac{a}{(B_t B_g)^{0.5}} - \frac{b}{E_g} \left( \frac{B_t}{B_g} \right)^{0.5} \quad (1)$$

where  $a$  and  $b$  are functions of the axial speed and the spreads in both initial axial and radial velocities, and  $B_t$  and  $B_g$  are the magnetic-focus fields at the tape and at the gun.

The negative sign implies that for certain values of the parameters, electrons with two different initial axial velocities will be brought to simultaneous focus. This is apparently analogous to the effect produced by color correction in optical lenses.

The diameter of the image of the crossover in the gun must be added to  $d$  above to obtain the total spot size.

A check of this expression by experiment requires an accurate knowledge of the velocity spread in the beam as it emerges from the limiting aperture. This check will be made as soon as the velocity spread can be measured at this point.

## SECTION II. PHOTOCONDUCTOR RESEARCH

### A. MODIFICATION OF TEST APPARATUS

Near the end of the previous contract\* work was undertaken to modify the two demountable test sets to permit both the scanning electron beam and the illumination to be incident on the same side of the target. These tasks have been continued under the present contract, and have consumed a substantial portion of the effort during this reporting period.

The required modifications to one of the test sets (Demountable "A") have been completed. This system employs an off-axis electron gun in order to leave clear a direct optical path for the incoming light. Also incorporated is a provision for illumination from either the insulator side or the base electrode side of the target. Thus complete evaluation of targets in both electrical polarities and with incident light from either direction can be performed. This versatility will be helpful in a number of ways, such as in the further investigation of electrode effects.

Developmental work on the other test set (Demountable "B") is still in progress. Difficulty is being encountered in the accelerated deterioration of test targets. It is thought that the damage is caused by excessive heat generated by the flood gun. Methods for correcting this condition are being sought.

In the past, incandescent illumination for tests of photoconductors has generally been supplied by a lamp operating at a color temperature of 2900°K or lower. A flash tube having a spectral distribution corresponding to 6000°K color temperature is being installed in demountable "A" in place of the 2900°K lamp. Calibration of the flash tube is in progress, and it is expected that the demountable system will shortly be operating with this light source.

### B. EFFECTS OF REVERSED DIRECTION OF ILLUMINATION

A number of targets previously tested with illumination through the base electrode were retested in demountable "A" with illumination incident from the scanned side of the target. The results are shown in Table II.

It can be seen that the sensitivities obtained with the signal plate positive (i.e., with field polarity in the photoconductor such as to move holes from the base electrode to the photoconductor-insulator interface) are in all cases substantially lower when the target is illuminated from the scanned side than when the illumination is introduced through the base electrode. This is because in the latter case effective photo-excited

\*Contract No. AF33(657)-8843

TABLE II. COMPARATIVE SENSITIVITIES OF SELECTED TARGETS  
FOR ILLUMINATION FROM OPPOSITE DIRECTIONS

Target	Electrode	Photoconductor	Insulator	Sensitivity (milliamperes per watt)*	
				Signal Plate	
				Positive (1)	Negative (2)
B633	SnO	As <sub>2</sub> Se <sub>3</sub> + Sb <sub>2</sub> Se <sub>3</sub>	Styrene	49.80	4.030
B618S	SnO	As <sub>2</sub> Se <sub>3</sub> + Sb <sub>2</sub> Se <sub>3</sub>	Styrene	57.30	0.855
B617	SnO	As <sub>2</sub> Se <sub>3</sub> + Sb <sub>2</sub> Se <sub>3</sub>	None	36.90	3.020
B617S	SnO	As <sub>2</sub> Se <sub>3</sub> + Sb <sub>2</sub> Se <sub>3</sub>	Styrene	32.25	3.135
B644G	Au	Sb <sub>2</sub> S <sub>3</sub> (Sb) + As <sub>2</sub> Se <sub>3</sub>	Styrene	6.24	2.82
					6.18
					23.8

(1) Illuminated through base electrode

(2) Illuminated from scanned (insulator) side

\*Incandescent illumination, 2900°K color temperature

carriers are generated in a narrow region of the photoconductor close to the electrode, and the photoconductor layer is strongly light-absorbing. When the target is illuminated through the transparent electrode, most of the incident luminous energy is available in the critical region and produces effective carriers. With the illumination incident from the opposite side of the target, the light must traverse practically all of the absorbing photoconductor layer before reaching the critical region; consequently only a greatly attenuated light beam is effective in producing photo-excitation. This explanation is supported by the fact that target B618S is about three times as thick as B617S (300 milligrams of photoconductor evaporated in B618S vs 100 milligrams for B617S). Qualitative observations of the relative optical densities of the tested targets are also consistent with this interpretation. Spectral sensitivity measurements for these samples have not been completed.

### C. PHOTOCONDUCTIVE GAIN OF "MIXED SELENIDES"

The principal emphasis in photoconductor research is being placed on developing an understanding of the mechanism of photoconductive gain in coevaporated layers of  $\text{As}_2\text{Se}_3$  and  $\text{Sb}_2\text{Se}_3$ . Several series of tests have been planned in which d-c measurements of "sandwich cells" of the mixed selenides will be employed to explore the properties of these layers in detail. Photocurrent-voltage characteristics over an extended range of applied voltage (or electric field in the photoconductor layer) are to be obtained to elucidate the physical behavior of the layers. Sensitivity as a function of composition in the range 0 to 50 percent  $\text{Sb}_2\text{Se}_3$  (in  $\text{As}_2\text{Se}_3$ ) will be investigated to determine the region of onset of the unusually high gains found previously in mixed-selenide layers. The spectral response of the different compositions will also be determined. Tests with evaporated gold electrodes are being conducted initially. It may be necessary to experiment with different electrode materials in order to obtain samples with suitable characteristics.

Considerable difficulty has been encountered in preparing usable sandwich cells for this work. Pinholes in the photoconductor layer caused short circuiting between the gold electrodes which is not a new problem; it has plagued many experiments attempting to evaporate electroded samples in the sandwich configuration. In the present case, it appeared at first that the pinholes in the mixed selenides developed after the photoconductor was deposited, during evaporation of the second gold electrode. After further examination it appeared that the roughness of the glass substrate surface was responsible. The use of substrates with optically polished surfaces apparently eliminated the difficulty. At this writing, several good sandwich cells have been prepared, and indications are that others can now be made at will.

Concurrent with development of techniques for preparing sandwich samples, a preliminary investigation of mixed selenide layers by the use of gap cells has been performed. The gap cells employed consist of a layer of 50 percent  $\text{As}_2\text{Se}_3$  and 50 percent  $\text{Sb}_2\text{Se}_3$  codeposited on gold electrodes having a gap 0.003 inch wide. The

current-voltage characteristics of such a cell are shown in Figure 5. Although there is considerable scatter in the data, the evidence strongly suggests that behavior, both in the dark and at high light intensity, is strictly ohmic over the range of fields from  $5 \times 10^2$  to  $5 \times 10^4$  volts per centimeter. (The apparently non-ohmic dark data, shown as Test No. 6 in Figure 5, does not represent steady-state conditions. The temperature of the sample varied during this run, and the sample had not been dark long enough to ensure equilibrium.) The indications of deviation from ohmic behavior at fields greater than  $5 \times 10^4$  volts per centimeter under high light intensity are unreliable, since it was found that the application of these high fields damaged the cell. The damage was evidenced by flaking and peeling of the photoconductor in the vicinity of the gap. Other gap cells of the same geometry and composition were damaged in the same way by fields ranging from this magnitude down to about  $5 \times 10^3$  volts per centimeter. It has been found that the damage starts at the edge of one electrode (i.e., along one side of the gap), and consequently it is believed to result from arcing at irregularities in the electrode edge.

A plot of the spectral response of a gap cell is shown in Figure 6, which also shows a plot of the response of a standard storage target for comparison. The curves have been separately normalized. The actual absolute sensitivity of the gap cell, in terms of photocurrent per milliwatt of radiation, is smaller than that of the standard target by orders of magnitude. The shift in response of the gap cell toward longer wavelengths probably results from the special geometry of the cell; in traversing the photoconductor layer parallel to the electrodes, light of shorter wavelengths is attenuated more rapidly than the long-wavelength light. Comparisons of these two samples of markedly different geometries are extremely tenuous. The same geometrical considerations must be carefully applied in other measurements, as for example in the intensity curves shown in Figure 7. The gammas for these data are considerably less than unity, much smaller than the gammas observed in standard storage targets.

It must be emphasized that these measurements of gap cells are interim experiments. Any attempt to correlate these results with Photo-Tape performance would be premature. Since sandwich cells are now available, the gap cell investigations will probably be discontinued.



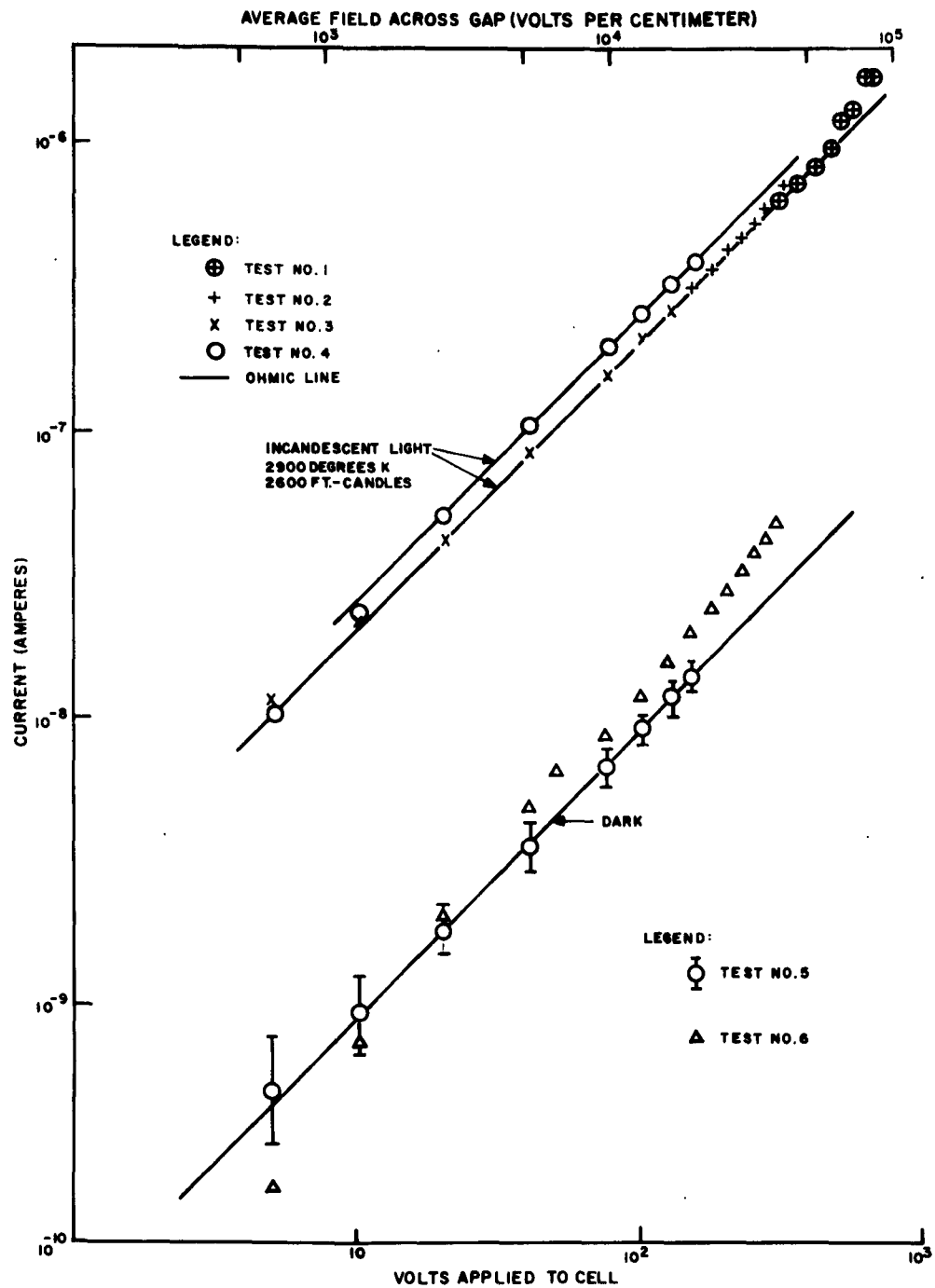


Figure 5. Current-Voltage Characteristic for Gap-Cell No. 1

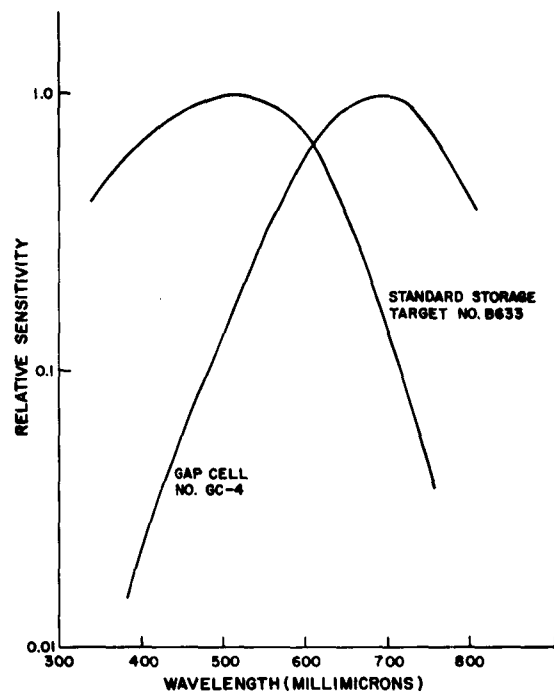


Figure 6. Spectral Response of Gap Cell and Standard Storage Target

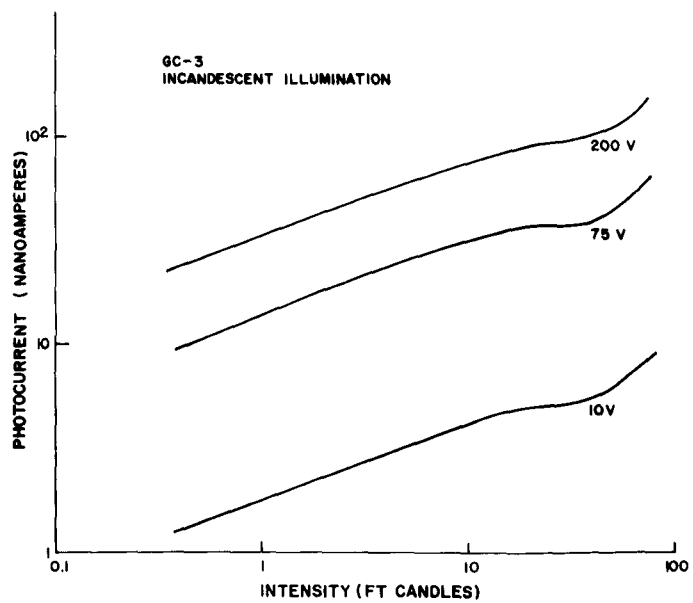


Figure 7. Variation of Response of Gap Cell with Light Intensity for Different Applied Fields

## SECTION III. ELECTRON-GUN RESEARCH

### A. INTRODUCTION

In the Photo-Tape system the properties of the beam are important not only for resolution, but also for sensitivity. The development of signal during readout is not the same as it is for the image orthicon or vidicon; it is not dependent on the replenishment or cancellation of the charge stored at the target. As in the image orthicon, an image is formed at the target as an electrical potential pattern, which is sensed by the probing electron beam, but in this case the potential pattern modulates the velocity rather than the amplitude of the return beam. (The return beam is velocity-analyzed to extract the signal.) The current in the return beam is directly proportional to the current in the high-velocity reading beam. The signal derived is proportional to the product of the electrical potential stored at the target and the incident beam current. It is interesting to consider the case in which the secondary emission ratio of the insulator target surface is unity and redistributionless readout is employed so that the potential pattern of the target surface does not change with bombardment by the reading beam. In this case the advantage of using higher beam current within a given spot size in order to increase sensitivity is conceptually limited only by the noisiness of the bombardment process.

The requirement for an electron gun design which provides high current density in a minimum spot diameter is strongly indicated. The electron gun program has set for its present goal the achievement of current density of one ampere per square centimeter with a beam spot diameter corresponding to 50 percent response at 50 cycles per millimeter. Present operation achieves a few milliamperes per square centimeter at the required spot size.

### B. CONVERGENT-FLOW PIERCE-TYPE GUN

The feasibility of utilizing a convergent-flow (Pierce Type) gun to obtain high spot current densities with low cathode current densities was studied. With the convergent flow gun, densities at the aperture of 30 times the cathode current density appear attainable. However, if the effect of increased velocity spread is included in the spot diameter at the target, a maximum increase of 6 times cathode current density is the practical limit. Such a gun would require an aperture of 0.7 times the diameter of the aperture required in the absence of velocity spreading. Because of this smaller diameter, the aperture current density will have to be twice that required at the target. The effective improvement at the aperture over cathode current density would, therefore, be only a factor of 3.

The cathode of such a gun would be 0.028 inch in diameter. The convergence angle would be 18 degrees. Providing focus electrodes with sufficient precision to establish convergent flow for a gun with these dimensions is expected to be difficult and expensive.

The convergent-flow gun will be considered further only if other less complicated guns fail to achieve the required level of performance.

### C. OTHER GUN CONFIGURATIONS

Other electron gun configurations show more immediate promise for attaining higher current density with high resolution. Experimental programs were instituted for several of these configurations.

#### 1. Triode Gun with Modified Spacing

This is a modification of the gun presently being used which gives current densities in the spot of several milliamperes per square centimeter but is capable of giving several hundred milliamperes per square centimeter.

However, the higher current densities are achieved only with less-than-useful resolution. An observed property of these guns has been that the spot size increases far less rapidly than the current density. In an effort to take advantage of this property, a gun has been fabricated in which the defining aperture has been moved approximately twice the normal distance away from the position where electrons cross the axis within the gun structure. This change is expected to result in the use of a smaller section of the crossover and to reduce aberrations. If the relationship between current density and spot size continues to hold for this modified gun design, it should be possible to achieve higher current densities in a usable spot diameter. A gun of modified design has been received and is currently being tested.

A shortcoming of the modified gun design is that the maximum obtainable beam current will be less than that of the standard gun. In order to increase maximum beam current it is necessary to increase the cathode current density capabilities beyond that of standard oxide cathodes. A gun design which incorporates this change is discussed below.

#### 2. Gun with Smooth Metallic Cathode

Tantalum and tungsten cathodes are capable of emission densities of nearly an order of magnitude larger than oxide cathodes. The higher emission densities of these materials should allow production of correspondingly higher spot current densities. These higher emission densities are associated with higher temperatures.

However, light emitted from the gun cathode during readout should not damage readout capability. Furthermore, the surfaces of these metallic emitters can be made extremely smooth by electropolishing them. Previous work on electron guns (Reference 2) has indicated the need for a smooth cathode surface to obtain improved resolution. Smoothing the surface of oxide cathodes increased the resulting gun resolution by nearly a factor of two over sprayed cathodes which were not smoothed.

A gun with a small directly heated tantalum cathode has been ordered for evaluation. It has not as yet been received from the tube shop. However, another preliminary evaluation of a possibly high-current density smooth cathode which could be operated at a lower temperature than tungsten or tantalum was started, using lanthanum-hexaboride for the emitting material.

### 3. Lanthanum-Hexaboride Cathodes

Lanthanum-hexaboride is being reexamined as a cathode material for high-current density on the basis of a recent report (Reference 3) which describes very high values of thermionic emission from polished single crystals of the fused material. A test diode with  $\text{LaB}_6$  fused on tantalum was fabricated. Results indicate that the emission work function was that of tantalum. Since boron diffuses rapidly into most metals at high temperatures, it was concluded that this had occurred during the fusing operation. The free lanthanum evaporates rapidly at operating temperatures.

A second cathode was prepared, which included a layer of tantalum-carbide over the tantalum base. The lanthanum-hexaboride was fused on top of this. It was hoped that the carbide layer would act as a barrier on boron diffusion and allow the emission properties of lanthanum-hexaboride to be measured. The surface was analyzed by X-ray diffraction techniques. No lanthanum was found to be present. The RCA Laboratories has prepared fused lanthanum-hexaboride on several different substrates both by direct heating and by electron-bombardment heating. If analysis of any of these indicates residual lanthanum, a test diode will be fabricated.

### 4. Phillips Cathodes

An electron gun has been designed to evaluate the Phillips cathode for use in a readout assembly. This cathode is supposedly capable of emitting several amperes per square centimeter, as compared to a few tenths of an ampere per square centimeter for the oxide cathode. The gun also includes a close-spaced aperture electrode, an anode, and a multiplier dynode.

The first gun of this type which was tested in a return-beam monoscope tube showed electron emission from the aperture electrode. The gun design also permitted electrons from the sides of the cathode to travel directly to the electron multiplier.

A second gun was built in which a remedy was sought for these defects. The first stage of the electron multiplier was insulated from the anode so that the latter could be used as a suppressor for electrons emitted from the aperture electrode. Holes which had allowed electrons to travel directly from the cathode to the multiplier were covered. However, this gun was damaged during processing when the aperture electrode was overheated and had a hole burned through it.

A third gun has been ordered with closer cathode-to-aperture electrode spacing to reduce the voltage necessary to obtain a given current density. In order to further reduce heating of the aperture electrode, the aperture diameter has been increased from 0.0004 to 0.0016 inch.

## CHAPTER III. DEMONSTRATION MODEL CAMERAS

### SECTION I. CAMERA I OPERATION AND COMPONENT TESTING

#### A. OPTICAL TESTS ON CAMERA I

Considerable effort on the Camera I support program has been channeled toward evaluation of the new optical system described in Monthly Status Report No. 2. Although individual components of the system have been tested separately (lens, vacuum and flood-gun windows, targets, etc.), the cumulative effect of all of these components on the final image on the tape under actual camera operating conditions has not been determined. This effect was observed when the electrostatic tape in the camera was replaced with a high-resolution photographic film, Type No. SO-243. This film type was selected because it has a high-resolution capability, with light sensitivity approximating that of the electrostatic tape. The characteristics of film Type No. SO-243 are identical to that of film Type No. SO-132. The sine-wave response curve of film Type No. SO-132 at high contrast is shown in Figure 8. Kodak data on film Type No. SO-132 indicates that although the resolution capability of this film is reduced by a factor of approximately two at two-to-one contrast range, it is still sufficient for the optical tests on Camera I.

Certain modifications were required on the Camera I enclosure so that the tape could be replaced with the film. A special fixture was constructed in the image plane of the camera to hold the film firmly in the focal plane, since electrostatic attraction could not be used with photographic film. The fixture consisted of a metal frame constructed in the form of a grid, which was placed in front of the platen and secured in the focal plane of the system. The film was threaded between the platen and the grid, and could be moved when the platen was retracted by an electromagnet. However, when the platen was released the film was pressed firmly against the reference grid, which provided uniform flatness across the field of the picture.

A considerable number of pictures were exposed under various conditions of illumination, exposure duration, focus-setting, vacuum, etc. The film was always developed in Kodak Type No. D-19 developer for eight minutes at 68°F. The major tests conducted on the system were as follows:

1. Evaluation of the focusing method,
2. Determination of the optimum focus setting of the lens,
3. Determination of the proper exposure for the highest resolution on the film,

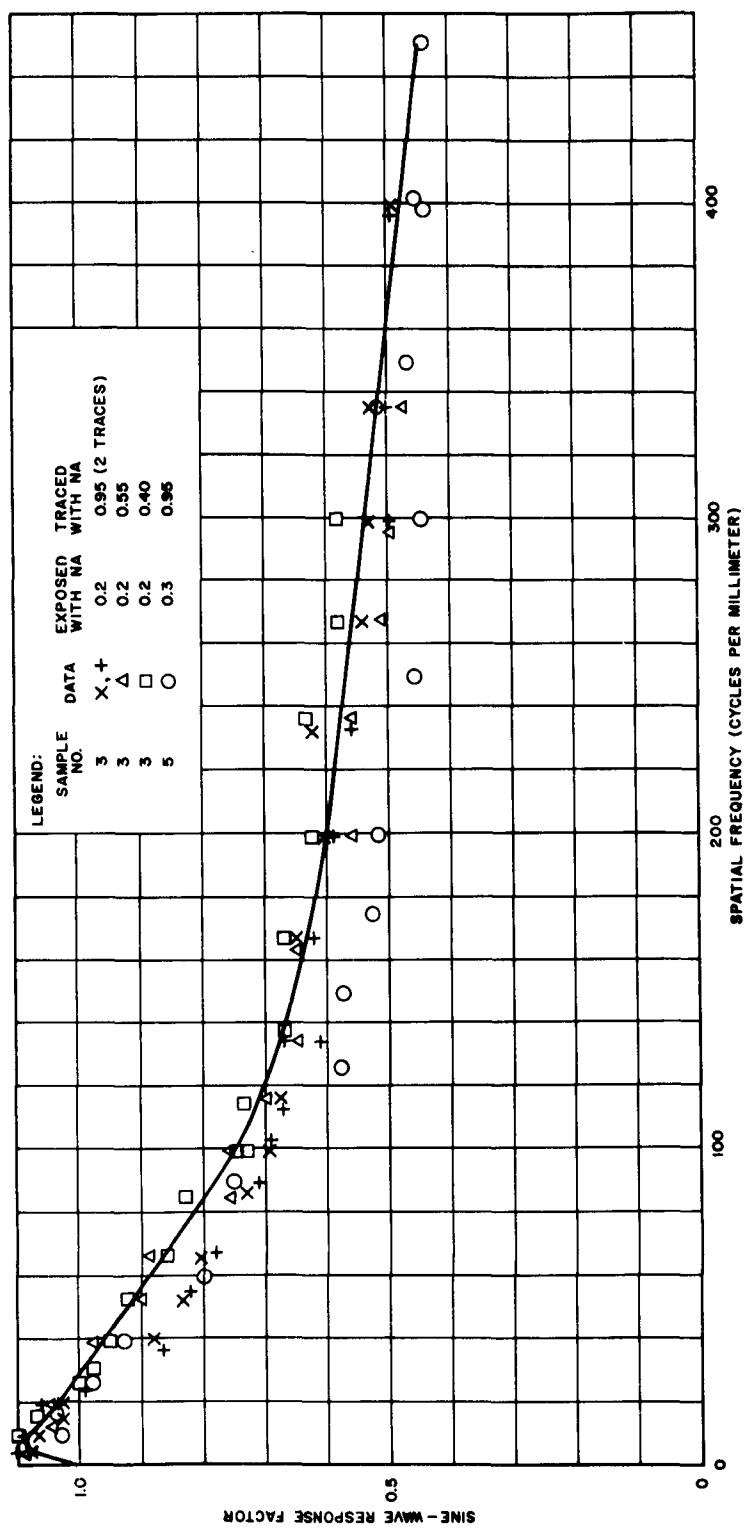


Figure 8. Sine-Wave Response Curve of Film Type No. SO-132 at High Contrast



4. Evaluation of the vibration of the complete camera assembly,
5. Investigation of platen reflectance,
6. Color correction of film response through reduction of the red portion of the optical input, and
7. Evaluation of vibration caused by the shutter motion.

As described previously, a special focusing arrangement was constructed on Camera I. The lens is focused with the aid of a microscope mounted behind the target, which looks through the lens system at a section of dielectric tape. The microscope is prefocused in the plane of the test target. The camera lens is then adjusted for optimum focus of the tape surface. This focusing arrangement was checked through the use of a second microscope, which was mounted within the camera enclosure in such a way as to provide a means of examining the image formed in the plane of the tape. Results of this evaluation indicate that exact axial-focus setting of the lens can be achieved in this way.

Photographic film was placed in the camera, and the focusing arrangement was further confirmed by exposing a number of pictures at various positions of the lens, which was moved about the optimum-focus setting in 2-mil steps. The test targets, in addition, were arranged so that they could be spaced at 1/4-inch intervals in the axial direction in front of and behind the optimum-focus plane, which resulted in effective one-mil deviation per step from the optimum focus in the image plane with 15.8-to-1 magnification in the optical system. Thus, even if the lens was not properly focused on the desired target, there would be at least one other target in the center of the field of the lens to provide an exactly focused image in the plane of the film, since the depth of focus of the lens was about two mils.

A proper exposure was determined for the highest resolution on film after optimum focusing of the lens was achieved. This was established by varying the exposure duration over a certain range, and selecting the setting that provided the most satisfactory resolution.

The system was evaluated with respect to the vibration that could have been transmitted through the structure. A number of pictures were taken at 1/400-second exposure and compared to those exposed at 1/25 second with reduced illumination. No significant difference in resolution was observed between the two types of pictures, indicating that there were no degrading effects due to vibration.

At this time it was noticed that the light transmission of the undeveloped film was about 25 percent. Consideration was given to the possibility that some of the light was being reflected back from the platen, reducing the resolution during exposure. The platen, therefore, was blackened to reduce reflection. Blackening of the platen apparently increases the resolution on photographic film. However, it is

difficult to evaluate the gain, since vertical and horizontal resolutions differ by almost 50 percent, with the maximum and minimum limits deviating above and below the average values that had been obtained previously.

Investigation of the spectral response of the film revealed that in the red portion of the spectrum, the sensitivity of the film was considerably higher than that of the electrostatic tape. It was assumed then that some of the degradation of resolution apparent on the photographs obtained could be attributed to the wider spectral range, which was not effective in the case of electrostatic tape. A series of pictures was exposed using a "minus-red" filter to eliminate this problem and to provide the same operating conditions for the lens that existed in the case of electrostatic tape. (Addition of the "minus-red" filter increases the limiting resolution.) However, the difference between horizontal and vertical resolution was still great.

The purpose of one of the final tests conducted with photographic film was to evaluate the vibration caused by shutter motion. Several pictures were exposed by use of a strobe-light instead of the shutter. The strobe-light experiment indicated that considerable degradation of resolution may take place with certain angles of illumination of the object.

Some of the most representative results were obtained from the photographic tests with the use of the "minus-red" filter which provided for maximum lens performance by avoiding chromatic aberrations. The results are shown in Table III. While no attempt is made at this time to explain some of the effects, several significant conclusions may be derived from the photographic data:

1. The present optical system configuration of Camera I will not be acceptable for Level-B performance.
2. It was noted that the limiting resolution obtained on the film is in the order of 60 cycles per millimeter. Taking into consideration the fact that the read-beam response was found to be about 45 percent at 50 cycles per millimeter during the measurements program, it can be stated that the over-all limiting resolution could not have exceeded the 45 cycles-per-millimeter value with the present optical system of Camera I.\*
3. Horizontal resolution is seldom equal to vertical resolution on a photograph taken from the same test chart.
4. Variations between horizontal and vertical resolution are random.

---

\*The term "optical system" is used in its broad sense to include all components of the subassembly such as the lens, test targets, light source, etc.

TABLE III. RESOLUTION DATA FOR PHOTOGRAPHS TAKEN WITH THE MINUS-RED FILTER

Frame No.	Horizontal Resolution		Vertical Resolution		Conditions	
	Contrast	Group	Cyc/mm	Contrast		Group
1	H	2, 6	102	H	3, 2	142
	L	2, 1	63.2	L	2, 1	63.2
2	H	2, 6	102	H	3, 2	142
	L	2, 2	71.0	L	2, 1	63.2
3	Underexposed					
4	H	3, 3	158	H	3, 1	126
	L	2, 3	79.6	L	2, 1	63.2
5	H	2, 6	102	H	2, 1	63.2
	L	1, 2	56.2	L	1, 1	31.6
6	H	3, 1	126	H	3, 1	126
	L	1, 6	56.2	L	1, 6	56.2

NOTES:

1. Exposure time is 1/200 second for frames 1 through 3 at f/5.6
2. Frame No. 4 exposure is 1/25 second at f/5.6
3. Frame Nos. 5 and 6 were taken with lens open using a strobe-light

## **B. READ-GUN TESTS**

Reassembly and modification of Camera I to incorporate the redistributionless read gun has been completed, including fabrication of another anode power-distribution chassis to provide the proper voltages to the eleven-stage electron multiplier. The addition of four stages necessitated rewiring the divider network to accept a higher working voltage range in addition to the installation of five extra outlets. The preamplifier was also slightly modified along with the ring voltage distribution system to accommodate the different voltage requirements and tube pin connections. A new current regulator, capable of supplying four separate outputs variable from 0 to  $\pm 225$  milliamperes, was installed for the alignment coils in the new gun.

During the vacuum pump-down with the redistributionless read gun installed, a crack developed around the tube base, apparently as a result of stress in the glass. Annealing problems during repair produced another crack in the tube neck. The read gun has been repaired and tests are being initiated.

## SECTION II. CAMERA II SYSTEM ASSEMBLY

### A. GENERAL

In view of the considerably higher level of performance established for the Level-B phase of the Photoconductive Photo-Tape Program, the presently available components of the camera system were analyzed to determine their limitations with respect to the new goals of the program.

The circuitry intended for use on Camera II is similar to that existing in Camera I except for some modifications of the individual components, which are described in Paragraph C of this Section of the Report.

### B. SYSTEM SPECIFICATIONS

On the basis of the analysis of the requirements for the Level-B performance, the following system parameters were established:

Resolution	85 cycles per millimeter
Bandwidth	8.55 megacycles per second
Horizontal scanning rate	1500 cycles per second
Horizontal blanking period	100 x 10 <sup>-6</sup> second
Vertical frame rate (three available)	12 seconds per frame 6 seconds per frame 6 frames per second
Vertical blanking period (two available)	200 milliseconds (slow rate) 20 milliseconds (6 frames per second rate)
Number of scan lines per frame (three available)	18,000 lines per frame 9,000 lines per frame 250 lines per frame
Format size	57-millimeter diameter

Three vertical scanning rates will be incorporated in the Camera II system. Initial work with the system will involve the 6 second-per-frame rate for general purposes. Increase in resolution capabilities of the camera will require higher scan-line density. Thus the 12 second-per-frame rate will be employed.

The 6-cycle-per-second vertical rate will replace the high-speed monitor that is presently used on Camera I. It is possible that the routine operation of the camera system can be simplified considerably by providing this extra feature, which would enable the operator to adjust the camera parameters without the necessity of switching to standard scanning rates. Another important consideration indicating that this mode may be very useful in camera operation is that the horizontal scanning rate remains constant in all cases, thus providing the same scanning velocity of the read beam across the tape. This is not true when the high-speed monitor is used for the camera adjustments.

One possible drawback of the 6-cycle-per-second rate may be found in the read-beam alignment technique, where somewhat higher speeds might be desired. This particular point will have to be evaluated during camera operation.

## C. CIRCUITRY

### 1. Video Preamplifier

The same type of high-input-impedance, transistorized preamplifier that was used on Camera I, shown in Figure 9, has been fabricated with a line-driver output stage added to drive a 50-ohm attenuator for use on Camera II. The driver stage provides signal inversion so that the preamplifier has unity gain from 20 cycles per second to 12 megacycles per second, but the output is now inverted. The 0- to 120-decibel attenuator between the preamplifier and the first a-c video amplifier will be used to match the read-gun output at a variety of read-beam currents.

The same shielding technique of driving the input coupling capacitor shield and preamplifier inner shield in phase with the input to minimize stray capacitance is followed. Actual mounting of the preamplifier will be completed when the read gun is received. Initial testing has been completed; final testing will be under actual input-loading conditions by modulating the output dynode current of the read gun.

### 2. Video Amplifier

The same type of shielding scheme used on Camera I has been utilized for the video amplifier stages for Camera II:

- a. Individual a-c video amplifier stages (20-db gain),
- b. Separate high-peaker stage (40-db high-pass filter),

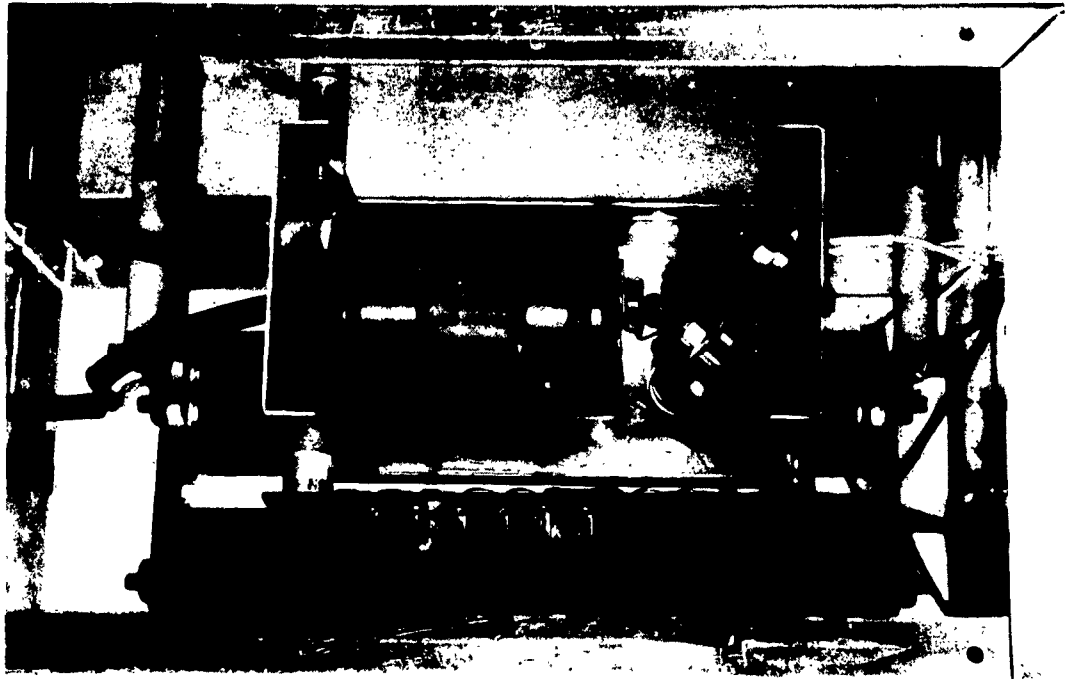


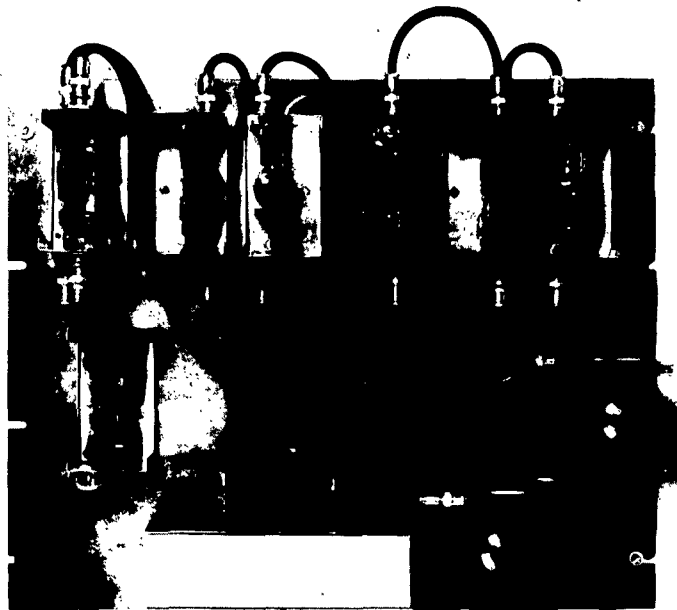
Figure 9. Video Preamplifier

- c. Separate d-c amplifier stage (20-db gain),
- d. Separate feedback clamp, and
- e. Separate output d-c amplifier stage (20-db gain).

Special copper shielding partitions have been added and are visible in Figure 10. Output line-driver stages have been added in the a-c video stages and high-peaker stage. Double signal inversion occurs in the a-c video stages, and single signal inversion occurs in the high-peaker.

All stages have been fabricated and are shown mounted in Figure 10, views A and B. Final wiring of input power from the system interlock has started.

Since the video amplifier uses the same power-supply voltages as the vertical-deflection, sync line, drives, one-frame readout, and other circuits which require the 30 volts from both "general supplies," the complete amplifier was tested with these circuits operating to simulate actual system operation. There were no problems in oscillations or cross-talk. The video preamplifier was operated from the same supply with no difficulty.



A. Front View



B. Rear View

Figure 10. Video Amplifier Stages, View A and B



The high-peaker was first tested separately and then within the video chain for a flat output (to 12 megacycles per second) with the input sweep signal to the video preamplifier rolled off at 20 decibels per decade above 100 kilocycles per second. The final evaluation of performance will be accomplished after the read gun is installed in the system, so that the test will be conducted under system-operating conditions.

### 3. Horizontal Deflection

The same type of transformer-coupled-output, horizontal-deflection circuit used on Camera I will be used on Camera II. This transformer has been built, rack-mounted, and tested driving the 4.6-millihenry horizontal winding of the original image orthicon yoke. The amplifier requires a separate +30-volt, 20-ampere, d-c power supply, and it will deliver 8 amperes, peak-to-peak, to the coil with a primary current of approximately 40 amperes, peak-to-peak. The amplifier will be located in the rack as close to its power supply as possible since power-line loss at 20 amperes and wire capacitance are critical. The output leads, approximately 20 feet long, will be a twisted pair to minimize radiation and pickup, and will be copper shielded to eliminate electrostatic pickup. Final testing with regard to linearity and 60 cycle-per-second interference will be performed following completion of assembly and integration. At present, it is known only that linearity is better than five percent, the limit of measurement with the oscilloscope. Centering is approximately plus or minus two amperes.

### 4. Vertical Deflection

Modifications to the vertical-deflection circuit have been completed and include:

- a. Addition of a selector switch to select sweep rates of 6, 1/6, or 1/12 frames per second,
- b. Addition of a potentiometer to adjust the slope of the 6-cycle-per-second saw tooth, to ensure the same amplitude of scan when switching between "high-speed" and "slow-speed" rates, and
- c. Changing reference-voltage values for centering to permit  $\pm 1$  ampere of centering.

The operation of the vertical deflection circuit in Camera II is, in general, the same as in Camera I, as described in the ASD Technical Report.\*

---

\*Final Report for Contract No. AF33(657)-8843

The output yoke leads were carefully selected. They were fabricated from a special four-conductor, twisted-interweave and copper-shielded wire, which is expected to minimize pickup. The vertical deflection circuit will be located within the electrostatically shielded rack mounted on an I-beam next to the read gun. Yoke leads will therefore be minimized in length (approximately two feet), and the resultant pickup of all frequencies higher than the vertical sweep frequency will be minimized to a greater degree than ever. Input power leads are also a twisted pair and are copper shielded, since power comes from the system interlock located in rack No. 2.

## 5. Control Circuitry

### a. General Description

A duplicate of the Camera I control circuitry, as shown in Figure 11, has been fabricated, rack mounted, and tested. Each parameter which must be variable is controlled by a ten-turn heli-pot. Two output test jacks are available for each control which provide monitoring of either output voltage or series current if both jacks are used. The control panel is located in rack No. 1 together with the variable-focus current supply. The read gun electrodes require static voltages since little current flows through output wiring. Consequently the need for twisted-pair shielded wire is not justified, and multiconductor wire with electrostatic shielding is being used. Additional filtering close to the read gun further minimizes pickup.

The control circuitry has been built, bench tested, and rack mounted, and system wiring has been started.

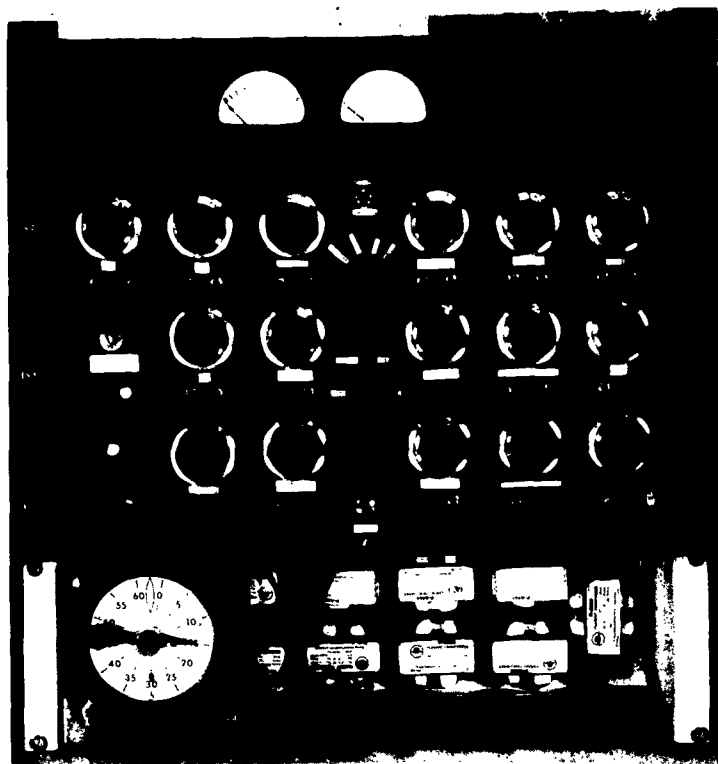


Figure 11. Control Chassis

**b. Flood-Gun Control**

Besides the ten amperes of current available for flood gun filaments which is controlled by an industrial timer through a powerstat, the control circuitry regulates the following elements of the flood gun and the tape:

1. Reflector,
2. Shield and  $G_3$ ,
3.  $G_1$ ,
4.  $G_2$ ,
5. Box, and
6. Tape Potential.

The  $G_1$  bias of the flood gun can be either manually controlled by a pushbutton switch or remotely controlled from the shutter or counter. Both the flood-gun cathode current and the flood-gun filament current are monitored by separate ammeters;  $G_1$  controls the amount and duration of cathode current, and the industrial timer and powerstat control the amount and duration of heater power. This power is usually not left on for any longer period of time than is necessary for preparing and exposing the tape due to the heat generated by the flood gun.  $G_1$  is maintained at -150 volts during the read and store cycles, while all the elements listed above, with the exception of the tape potential, are maintained at zero volts. The tape potential is connected to respective regulators during the read, write, or prepare cycles.

**c. Read Gun Control**

The control circuitry also provides voltages to the following elements:

- a. Rings 1 through 5,
- b. Wall,
- c.  $G_2$ ,
- d. Shield,
- e. Persuader, and
- f.  $G_1$ .

Normal potentials are applied during the prepare and write cycles with the exception of  $G_1$ , which biases the tube off on all cycles except read. During the read operation  $G_1$  may be connected to the preselected bias level either manually or by remote control; for the read operation it is connected continuously.

A one-frame readout device has been added to the system, which controls the cathode and is capable of (1) turning the read gun off indefinitely, (2) turning the read gun on for continuous operation, or (3) turning the read gun on for one frame only.

All elements except  $G_1$  are tied to ground through some resistance during the write and store cycles.

#### 6. Sync Generator

Fabrication of the sync generator in accordance with the design employed on Camera I, has been completed. The unit has been integrated with the line drivers and tested for proper pulse-width outputs. The sync generator utilizes a slightly different design for the 100-kilocycle clock, which will be tested for jitter along with the sync generator.

#### 7. Exposure Control (Shutter Delay)

Fabrication of the shutter-delay has been completed, and the unit has been modified as necessary and tested. Sequencing and timing signals to the shutter and the flood gun are provided with greater accuracy and flexibility on Camera II than on Camera I. The greater portion of the design utilizes plug-in boards\* that provide the logic. A control panel and emitter followers are designed and fabricated to provide control of timing and sequencing.

Operation of the shutter delay is based on a seven-stage binary counter that provides an output when the counter has counted down from some preset number to zero. If the states of the flip-flops of the counter are properly defined, i. e., when pin 6 is negative the state is zero, the resulting binary number is read from input to output.

The delay is equal to the waveform period of the input, times the binary number. The state of the flip-flops can be set by bringing in a trigger, prior to counting, to the appropriate side of the flip-flop. The time delay is then variable from zero to the maximum given by

$$\sum_{1}^{7} 2^6 = 127 \text{ clock periods.}$$

In the shutter-delay unit, during the first count cycle, the last stage is set to zero as a provision against false triggering. This makes an effective six-stage counter out of the unit, with a maximum delay of 63 clock units. The first delayed trigger

\*"Logix Blocks," manufactured by Reese Engineering Co.

is utilized to set the flip-flops for the second countdown, which has a maximum delay of 127 clock periods. Two sets of toggle switches provide the means of selecting the "state" of the flip-flops and thereby the delay.

Certain minimum delays other than the theoretical zero-time capabilities are used to allow for delays in associated circuitry. The extreme values for the delays are shown in Table IV; all delays are variable in 10-millisecond steps between these limits.

TABLE IV. EXTREME VALUES FOR SHUTTER DELAYS

Delay	Minimum (milliseconds)	Maximum (milliseconds)	Notes
<u>Negative Shutter Off</u>			
Shutter delay	5	635	From initial flood gun to shutter impulse
Continuation of flood gun	15	1285	From shutter impulse to end of flood beam
Total flood gun duration	20	1920	
<u>Negative Shutter On</u>			
Flood gun delay	15	645	Shutter impulse to initial flood gun
Flood gun duration	5	1275	

#### 8. Shutter Drive

The shutter drive, shown in Figure 12, is used to drive the "Ledex" rotary solenoid that operates the shutter on the camera lens.

The solenoid drive contains the following four circuits: (1) power supply, (2) pulse inverter, (3) "one-shot" multivibrator, and (4) power output stage.

Since this unit has a very low duty cycle, a small (1 ampere) self-contained power supply is used. The power supply charges the two 2,000-microfarad, 50-volt capacitors to the peak value, 45 volts. The capacitors supply a short (25-microsecond), high-current (7-ampere) pulse through the power output stage to the solenoid.

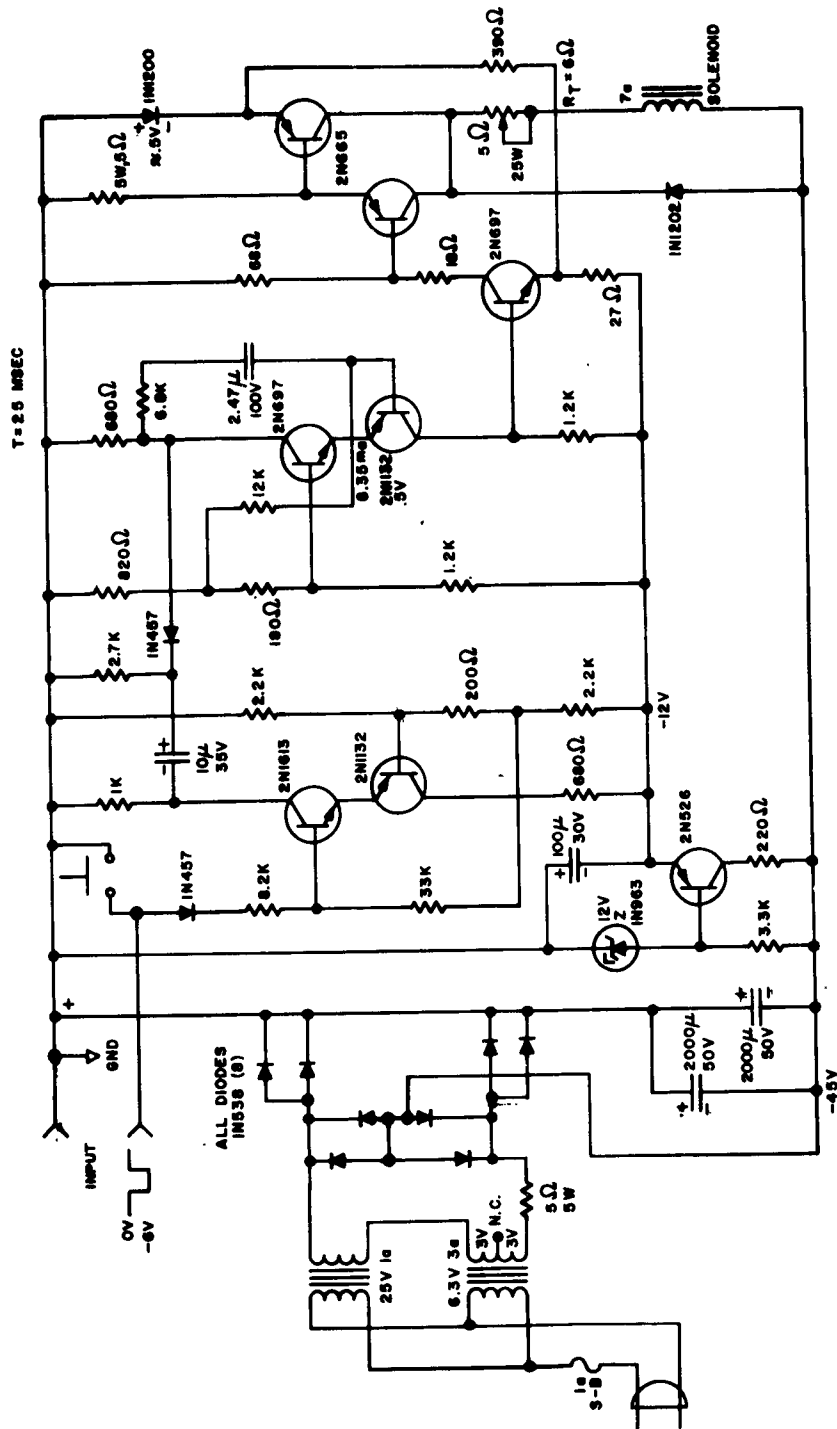


Figure 12. Shutter-Drive Circuit, Schematic Diagram

## 9. Alignment Coil Current Regulators

The alignment coil current regulators, floating at  $G_2$  potential, are for the four etched coils within the read-gun envelope, which are used to align the read beam. The four current regulators basically constitute a d-c to d-c converter, operating from -30 volts at half the horizontal rate so that switching occurs during blanking time. Through a transformer with the center tap returned to  $G_2$  potential, nine volts are developed, after filtering, to operate the regulators, which are capable of delivering  $\pm 225$  milliamperes to the coils. The complete coil current regulator chassis houses four separate regulators and has been mounted in the video amplifier and deflection assembly located on the optical bench. Final tests will be made when the read gun is installed.

## 10. One-Frame Readout Circuit

The one-frame readout circuit is the same as that used on Camera I, except for the addition of a relay and an indicator lamp to provide a visual indication of read gun bias conditions. The circuit itself generates a negative 6-volt pulse to energize one of the three diode inputs of an input "or" gate within the blanking amplifier, which causes the cathode to go to a positive 60 volts and cut off the read gun. The other two gated inputs are provided for vertical and horizontal blanking.

The circuit has been rack mounted and tested at both the slow-speed vertical rate and the higher rate of 6 frames per second.

## 11. System Interlock

The system interlock, pictured in Figure 13, has three purposes:

- a. To energize and de-energize the system with one easily accessible switch,
- b. To de-energize the system in the event of failure of an integral supply voltage, and
- c. To aid in troubleshooting faulty supplies.

The system for Camera II has been redesigned to add relays to control voltages and to minimize ground loops and interference, in accordance with the plan explained later in the assembly layout discussion. Since the interlock is a control center for nearly all system d-c voltages, the shielding of each voltage wire within the interlock and the addition of another ground-return wire for each supply (rather than one common ground) will provide controlled return paths and minimize ground loops. A schematic diagram of this system is shown in Figure 14.



Figure 13. System Interlock

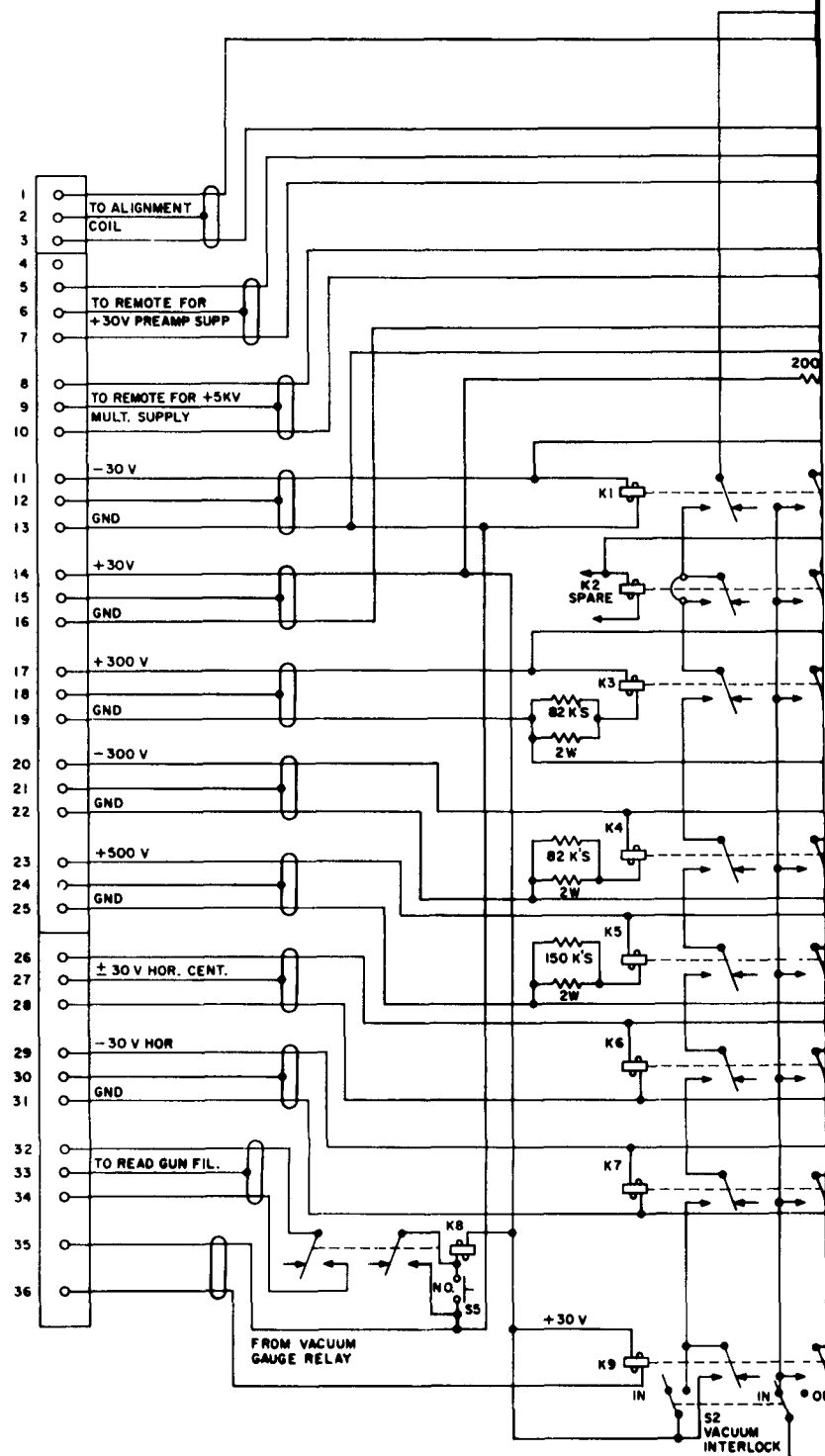
Because interlock control is not available with the new vac-ion pump, a circuit has been designed to energize a relay if the vacuum environment should fall below some predetermined minimum, e.g.,  $10^{-5}$  torr. This is necessary primarily to prevent damage to the read-gun filaments, since the filaments are kept on continuously; in the absence of vacuum during the night, the filament supply should be de-energized. This will also be interlocked to the system which will also be de-energized if vacuum decreases below  $10^{-5}$  torr.

Certain supplies, such as the preamplifier voltage supply and the dynode high voltage supply, are energized by the interlock but are not truly interlocked to shut off the system if they are not "on." The outputs of all other system supplies are switched to the required circuits through relays when the system "on" button is pushed, and in the absence of any one of the system supplies none are switched.

A main a-c control switch, to be used for emergency purposes and to energize or de-energize line-voltage supplies to all a-c units, will be installed.

The interlock contains a total of 22 relays, of which all require 6.3 milliamperes and 30 volts d-c. All indicator lights are neon lamps, which operate from the -300-volt supply with the exception of one 28-volt lamp utilized to indicate the presence of -30 volts.





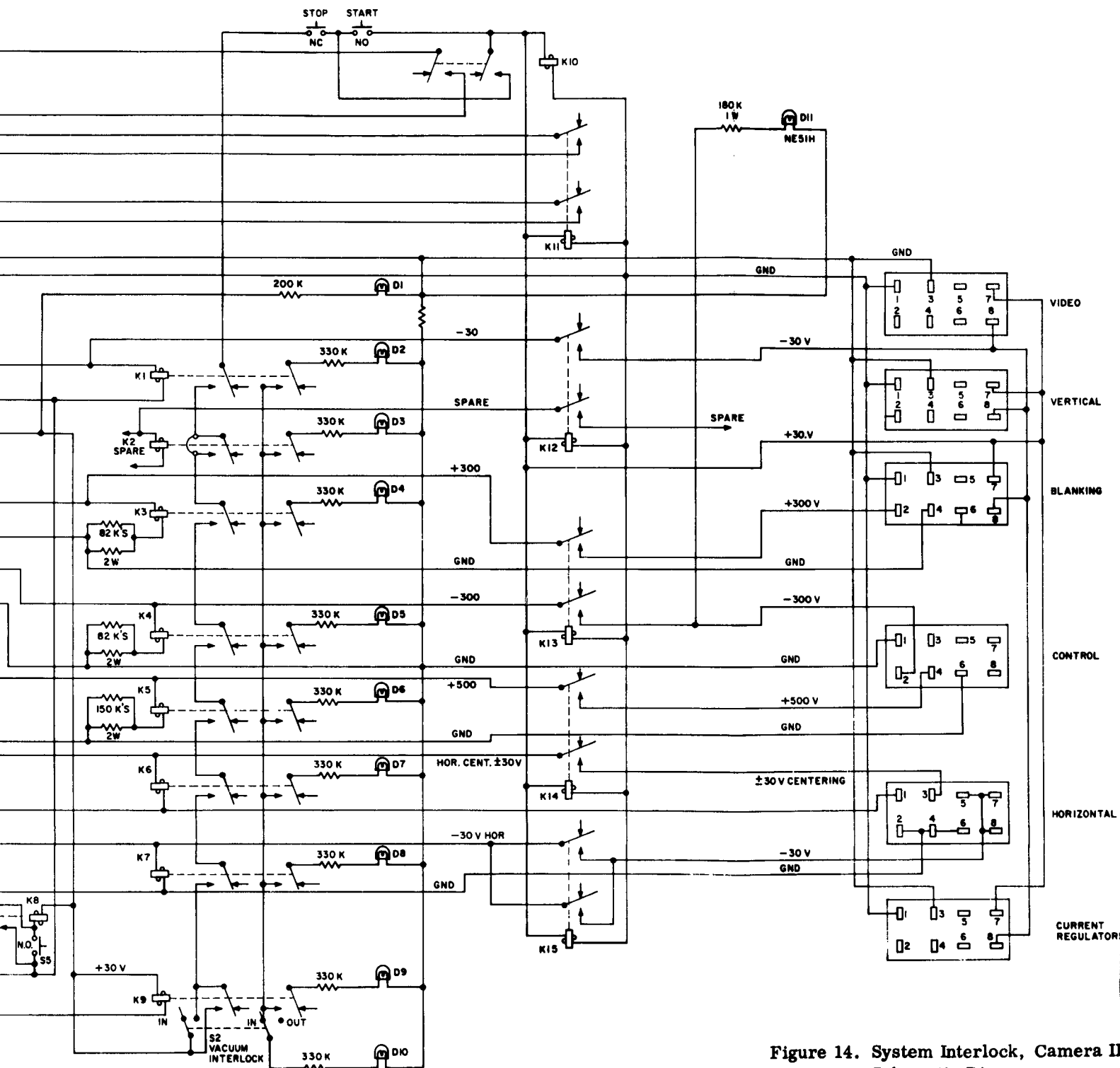


Figure 14. System Interlock, Camera II, Schematic Diagram

## 12. Focus-Current Supply

The focus-current supply\* is a high-precision, constant-current device, designed to furnish preset current levels in the range from 0 to 1 ampere at terminal voltages from 0 to 100 volts. The current level is set by means of a full-scale selector and a six-digit multiplier with in-line readout, thus providing resolution of one part per million of the full-scale value.

Since the focus-coil impedance is relatively high, the focus-current supply "runs out" of voltage, and another voltage supply\*\* is connected in series with the focus-current supply to provide the extra voltage. Table V provides the specifications for the focus-current supply, and Table VI provides the specification for the extra-voltage supply.

## D. ASSEMBLY LAYOUT

In order to optimize performance of the read gun and to minimize interference, assembly space for critical camera circuits has been provided directly on the optical bench, which also supports the camera housing and the read gun. This assembly location is referred to as the video amplifier and deflection assembly. Other circuits not critical in this location, as well as power supplies which should be remote from the read beam, constitute the power supply and control assembly. A brief discussion of these two assemblies follows.

### 1. Video Amplifier and Deflection Assembly

The video amplifier and deflection assembly includes the following components:

- a. Complete video amplifier,
- b. Vertical-deflection generator and amplifier,
- c. Cathode-blanking amplifier,
- d. Demountable read-gun electrode voltage supply,
- e. Demountable read-gun dynode voltage supply, and
- f. Preamplifier power supply.

The copper plate on all sides of the assembly box will be the common grounding point for the system.

---

\*Model CS-128, manufactured by North Hills Electronics

\*\*The extra voltage is supplied by a Model 1250B Kepco supply rated at 1000 volts at 500 milliamperes.

**TABLE V. SPECIFICATIONS FOR FOCUS-CURRENT SUPPLY**

<b>Stabilized output current</b>	0 to 1 amp
<b>Resolution</b>	5 ppm
<b>Current setting</b>	4 full scales: 1 ma 10 ma 100 ma 1000 ma  6-place multiplier, Ext. and 0 settings
<b>Load voltage</b>	0 to 100 volts, 115 line voltage
<b>Typical regulation</b>	0.0025% at 1000 ma from 0 to 50v
<b>Line regulation</b>	0.0025% at 1000 ma from 105 to 125v, a-c input
<b>Accuracy</b>	0.02% of full-scale setting
<b>Stability</b>	0.002% short term 0.01% long term
<b>Ripple</b>	0.01% or 0.01 ma, rms

**TABLE VI. SPECIFICATIONS FOR EXTRA VOLTAGE SUPPLY**

<b>Output voltage d-c</b>	0 to 100 v, continuously variable
<b>Output current d-c</b>	0 to 500 ma, continuous duty
<b>Regulation</b>	Less than 0.1 v for load variations from 0 to maximum current  Less than 0.2 v for line fluctuations from 105 to 125 v
<b>Ripple voltage</b>	Less than 3 mv, rms

The vac-ion pump ground which connects mechanically to the camera housing, will be tied electrically to the copper assembly system ground. Because the vac-ion high-voltage supply (5000 v) is now connected to a transformer (220 volt a-c) separate from the camera electronics, it will be necessary to disconnect the present vac-ion transformer ground. This ensures a common a-c power ground for a minimum 60-cycle-per-second interference. A scheme of separating power supply grounds and video, or signal, grounds (described in the following paragraph) will be utilized.

## 2. Power Supply and Control Assembly

In order to minimize magnetic pickup and/or radiation, shielded, twisted-pair wire is used for all power-supply leads. In order to ensure maximum cancellation of fields produced on a twisted pair, the same amount of current must flow on the "hot" wire as on the return wire. This requirement dictates controlled return paths and is accomplished by floating each chassis and supply, and grounding only one end of the external electrostatic shield. This was not done on Camera I, where a rack ground was often the return path for supplies, and twisted-pair wire was not used. It is unavoidable that certain chassis must be tied together and cannot all float. In this case, where signals must be coupled from one chassis to another, shielded coaxial cable is used with the shield grounded at both ends of the cable to provide the shortest signal ground or return path. This scheme was tested during checkout of the sync rack together with the video amplifier and vertical deflection circuits. The noise of the video amplifier and video preamplifier were completely free of crosstalk. Also, line-driver outputs were free of other pulses which have previously been a problem on Camera I. This problem existed because the same four voltages (+12, -30, -18, and -6 volts) were used on eight chassis. The problem was eliminated by providing a separate ground return within a shielded twisted pair for each voltage. The scheme for providing the same voltage to two lamps on separate chassis is illustrated in Figure 15.

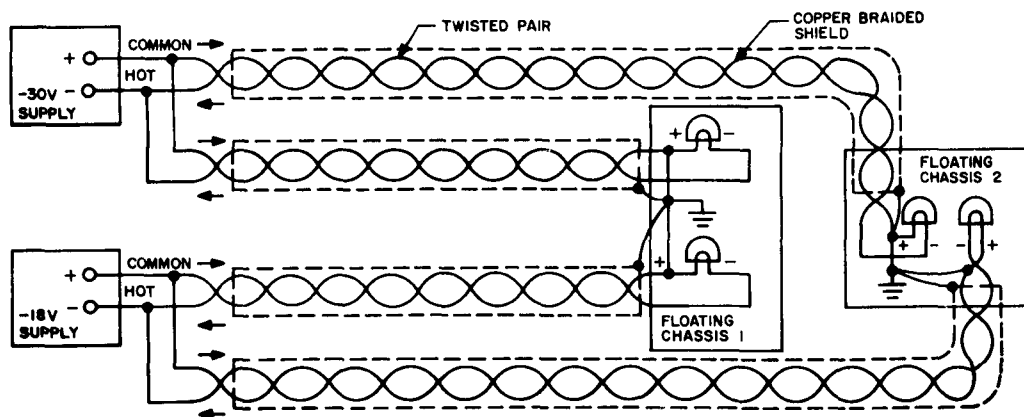


Figure 15. Scheme for Minimizing Ground Loops and Optimizing Magnetic Cancellation

The four relay racks located remote from the camera housing constitute the power supplies and control assembly. These racks are bolted together. Rack No. 1 houses all controls and is easily accessible to the operator. Rack No. 2 houses the horizontal deflection, the interlock, and all other system power supplies that require interlocking. Rack No. 3 contains digital circuitry only. All available supplies and chassis are mounted, and system wiring is progressing. A fourth rack has been added for test equipment and to provide additional space.

## **E. INTERFERENCE ANALYSIS**

### **1. Jitter**

The jitter may possibly be defined as a high-frequency magnetic-field disturbance within the read-gun structure that causes deviation of the read beam from its desired position during the scanning process. The disturbance is usually of a random nature, although in certain cases it may be periodic.

A disturbance of this type may be caused by various factors inherent in the system. Basically, the problem can be divided into two categories:

- a. Magnetic disturbance caused by some external field around the read-gun structure, and
- b. Instability in the circuitry associated with deflection components of the camera.

The magnetic-field problems associated with the external environment of the read gun are usually reduced, in the case of jitter, by shielding the yoke structure. The solution in this case is simple. By virtue of the high-frequency nature of the disturbance it can be considerably attenuated with a modest amount of shielding material.

However, jitter for the most part is usually associated with the circuitry employed in deflection components of the camera. There are two basic circuits that must be evaluated from the standpoint of jitter: the sync generator and the deflection circuit.

Basically, the stability of the synchronizing pulses should be of such high quality that any period difference between two successive pulses is only a small fraction of a resolution element of the system. In practice, however, the sync jitter may have a greater or lesser effect, depending on the particular system configuration. In the case where the video recording equipment is located in an area remote from the camera system, the problem may be extremely difficult when the sync information has to be recovered in the presence of noise. The present camera and recording apparatus utilizes a "triggered system" for control of the scanning rates of both units. The deflection circuitry of the camera and the recording device are triggered simultaneously from the same synchronizing generator under these conditions, so

that the effect of jitter is reduced to a point where it becomes academic. However, in view of the general system evaluation, certain tests have been performed on the sync generator to determine its performance capabilities with respect to stability.

The effect of read-beam jitter between any two successive resolution elements on the tape is to degrade the resolution performance of the system. The degree of degradation depends on the jitter amplitude, and its effects are being theoretically evaluated at present. It is assumed, for the present, that the maximum tolerable peak displacement of the read beam is 1/4 of one cycle. The required sync stability under these conditions then becomes 1/4 of one cycle within one horizontal period (667 microseconds), or 29.4 nanoseconds.

Attempts have been made to measure the jitter in the sync generator. The obvious method is to use an oscilloscope with a delayed trigger and to trigger on the leading edge of one pulse while looking at the leading edge of the next. Unfortunately, the best delayed-trigger module available has an inherent jitter. The manufacturer specified that this jitter is not to exceed 1 part in 20,000, but for a delay of 667 microseconds, which is the time between successive leading edges, this amounts to 33.3 nanoseconds, which is slightly larger than the tolerable sync jitter itself. Therefore the oscilloscope must be calibrated and cannot be used directly.

The calibration procedure consists of feeding the output of a 100-kilocycle, oven-controlled crystal oscillator into the oscilloscope, delaying it for 667 microseconds, then observing the jitter in the presentation. The jitter in the crystal oscillator, being typically better than 1 part in  $10^6$ , or 0.01 nanosecond at 100 kilocycles, could be considered negligible, so that any jitter in the scope presentation would be entirely that of the scope.

Results obtained from the measurements thus far indicate that the sync jitter is not greater than 30 nanoseconds. The exact jitter magnitude will have to be measured with a different type of apparatus.

Arrangements have been made with Polarad Electronic Instruments Corporation to attempt the sync jitter measurement using their Model PJ-1 Pulse Jitter Tester which is purported to have a resolution of less than 5 nanoseconds and an inherent jitter of about 0.5 nanosecond. It is hoped that this instrument will provide desired data with the accuracy sufficient for the Level-B evaluation work.

Stability requirements of the deflection circuitry may be evaluated in the following manner:

For the case of a 57-millimeter sweep across the tape, the total number of cycles at 85 cycles-per-millimeter resolution is

$$(85)(57) = 4.85 \times 10^3 \text{ cycles per line.}$$

If it is assumed that the beam will not be deflected by the noise in the deflection current by more than 1/4 of a resolution element, then the peak disturbance (deviation) of the deflection current should not be greater than one part in

$$(4)(4.85 \times 10^3) = 1.94 \times 10^4.$$

The rms value of noise under these conditions should be below the peak value of the deflection current by the factor of

$$(6)(1.94 \times 10^4) = 1.16 \times 10^5.$$

This shows that the signal-to-noise ratio of the current in the output of the deflection circuit has to be

$$\frac{S_{\text{peak}}}{N_{\text{rms}}} = \frac{1.16 \times 10^5}{1} \quad (2)$$

Expressed in decibels, this indicates that the rms noise component has to be 100 decibels below the peak signal (sawtooth) amplitude at the output of the deflection circuit. It is obvious that performance of this quality can be achieved only with sophisticated circuitry.

The present horizontal-deflection circuit has been analyzed from the standpoint of the signal-to-noise ratio of the output current. It has been assumed throughout the analysis that the major noise component in the signal is due to the thermal contribution of the impedance at the input of the sawtooth generator. The circuit at this point consists of a capacitor grounded on one side with the other side connected to the constant-current generator that is used to develop the sawtooth signal. The impedance of the capacitor changes from about 400 ohms at 1500 cycles-per-second to about 3 ohms at the upper end of the passband that is required for linear reproduction of the sawtooth. The computations are approximated by assuming a flat noise characteristic of a 100-ohm resistor at the input.

The rms noise signal is determined from the equation

$$E = (4KTBR)^{1/2} \quad (3)$$

where

$$K = 1.38 \times 10^{-23} \text{ joules/}^\circ\text{K (Boltzmann's constant)}$$

$$T = 300^\circ\text{K}$$

$$B = 500 \text{ kc (bandwidth of the circuit)}$$

$$R = 100 \text{ ohms (equivalent resistance at the input)}$$



From the above values, the noise component is found to be

$$E_{\text{rms}} = 9.1 \times 10^{-7} \text{ volts rms.} \quad (4)$$

The sawtooth amplitude developed across the integration capacitor is

$$V_{\text{sig}} = 10 \text{ to } 15 \text{ volts peak-to-peak.} \quad (5)$$

Thus peak signal to rms noise ratio under the above conditions is

$$\frac{S_{\text{p-p}}}{N_{\text{rms}}} = 10^7 = 140 \text{ db} \quad (6)$$

There are two transistor stages that may contribute to the noise degradation of the signal. Assuming the noise figure of 20 decibels is for the two stages for the "worst-case" analysis, then the output signal-to-noise ratio is expected to be

$$\left(\frac{S}{N}\right)_{\text{output}} = 140 - 20 = 120 \text{ db} \quad (7)$$

Analysis of the vertical-deflection circuit indicates that its performance should be considerably better than that of the horizontal-deflection circuit since the bandwidth of this circuit is much lower.

The preceding discussion indicates that although performance of the desired quality is possible under certain conditions it is marginal, with theoretical limits set by the system requirements. It is possible that some modification of the circuitry may improve the signal-to-noise factor by another 20 decibels. It should be noted, however, that only one type of noise interference has been considered in the above analysis, and that it might be desirable to limit the beam jitter to a smaller value than 1/4 of a cycle, a factor that would obviously prohibit any further increase in cycle-density per scanning period.

Similar reasoning also holds for the field stability in the vicinity of the read gun; i. e., the rms disturbance of the magnetic field within the envelope of the read gun, caused by fields external to the yoke assembly, should be 100 decibels below the peak-deflection field. This is a somewhat trivial problem at high frequencies, as indicated previously. Conversely, lower frequency interference may present a formidable task of shielding, as discussed later in this report.

## 2. Hum

Hum is defined as a low-frequency disturbance of the magnetic field within the read-gun assembly. Contrary to jitter, this type of disturbance is usually of a periodic nature. The problem may be associated with the circuitry, or it may be caused by some external field in the vicinity of the read-gun structure.

The circuitry problems associated with hum usually result from power-line ground loops. This requires careful grounding techniques, and it is assumed that a problem of this nature can be eliminated by proper assembly of the units.

The hum problems that are associated with external field disturbances, conversely, present considerable difficulties at low frequencies. Since the present peak value of the deflection field is about 80 gauss, the maximum tolerable rms deflection field "noise" should be below  $8 \times 10^{-4}$  gauss if the maximum peak jitter is to be below 1/4 of a cycle. A plot of a residual field for some of the best shielding materials is shown in Figure 16. It can be seen from the data that very high attenuation of the fields can be obtained at high values of flux. The curves flatten out, however, at lower values of input flux resulting in very low attenuation at flux densities of about 0.001 gauss. The above computations indicate that residual fields should be approximately an order of magnitude below that indicated by the plots. Considerable effort will be required to provide the desired results. This situation differs from that of high frequency, where the majority of the problems are contributed by the circuitry.

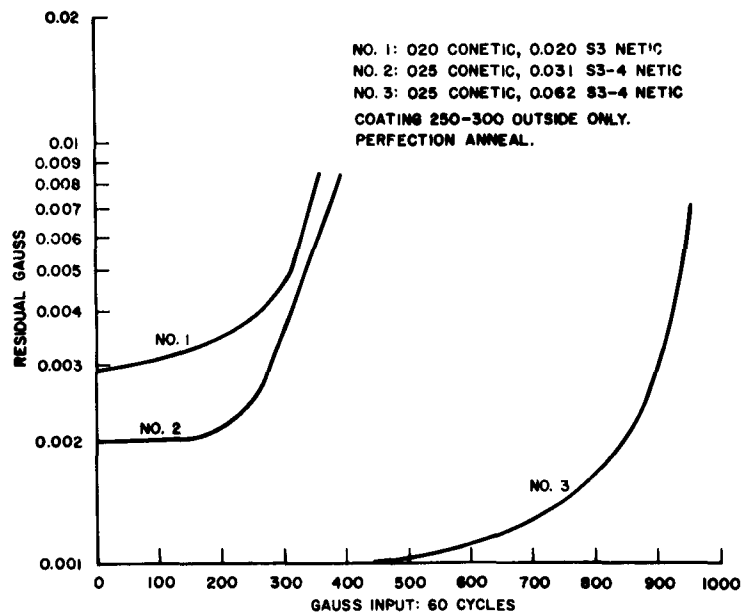


Figure 16. Saturation Curves for Two-Layer Material, Coated Outside Only

## SECTION III. SUBSYSTEM DEVELOPMENT

### A. CAMERA II ENCLOSURE MODIFICATIONS

#### 1. Negator Brake

The results of mechanical tests performed with the tape-transport mechanism have shown the need for a safety device to prevent the negator springs from suffering a whip-lash effect in the event the tape breaks or pulls loose from the reel hub, thus allowing the powerful springs to unwind from the power drum and onto the take-up drums. The flywheel action of the unrestrained reels would cause the system to accelerate and consequently impose a severe strain on the spring attachment to the power drum as it unwinds. The strain usually results in spring breakage.

An emergency brake has been designed to circumvent this possibility. The brake details are shown in Figures 17 and 18.

The drum-retaining screw has been replaced with a threaded stud. A mating, threaded bushing is attached to a cross bar which is loosely coupled to the tape reel by means of a sliding fit to shaft extensions on two of the take-up drums. The threaded bushing ascends or descends the central stud as the springs wind or unwind. A brass brake disc is attached to the upper flange of the power drum and mates with a stainless steel counterpart attached to the threaded bushing assembly. As the springs are concentrically wound on the power drum, the upper brake disc moves away from the lower disc. When the springs unwind, the upper disc approaches the lower and applies braking action to lock the two reels together when the springs are completely unwound. The locking action prevents further movement of the tape reel and its attached take-up drums, with respect to the power drum; therefore any strain on the spring is avoided.

A feature of the design is the incorporation of a locking pin to enable the operator to lock the spring tension at any point in the winding cycle during the tape loading operation.

Parts have been designed so that they can be integrated with the existing mechanism with a minimum of reworking.

Dissimilar metals have been used for brake discs to avoid the outgassing problems usually experienced with non-metallic materials.



Figure 17. Emergency Brake for Tape-Transport Mechanism

## 2. Electrostatic Platens

The platens have been insulated so that they may be charged with 1200 volts, d-c. The charge attracts the tape and tends to flatten it, thereby improving resolution. The voltage is applied during the write and read operations only.

## 3. Magnetic Plug

A new magnetic plug, used to maintain parallelism of the magnetic lines from the read-gun yoke during their course through the photo tape, is being designed. It will consist of 3/8-inch thick ferrite magnet material with a movable center section, the same size as the platen. The movable section will carry the platen and will be attached to the linkage system so that it can be used to press the tape against the aperture plate.

Since ferrite core material is both hard and brittle, it is difficult to work. It is not available in a size large enough to make the plug in one piece, therefore, it is planned to make the 6.4-inch-diameter disc in four sections. The need for slits complicates the construction. Non-magnetic, stainless-steel, discs will be used to form a laminated structure with the core material; the discs will both strengthen and bind the sectors together.

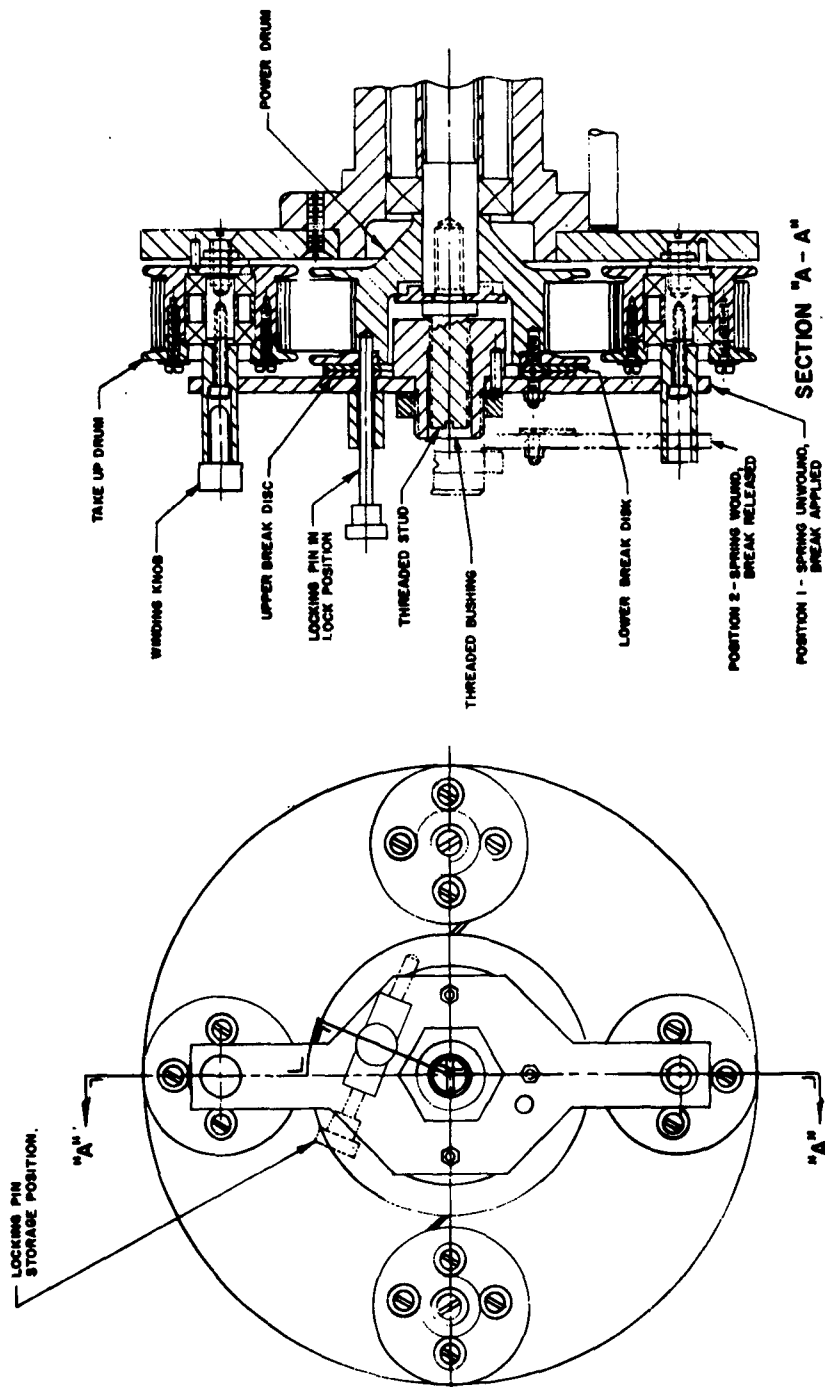


Figure 18. Emergency Brake for Tape-Transport Mechanism, Orthographic Projection

#### 4. Tape Guides

The revised magnetic plug design has made it possible to transfer the tape guides in the read position from an integral mounting with the aperture plate, to a mounting on the plug structure. This will improve the tape threading operation. The tape guides will employ teflon shoes to support the tape along its folded edges. This change of material will reduce friction and avoid scratches on the back of the tape.

#### 5. Aperture Plate Brace

Stiff braces anchored to the base plate have been provided to brace the write-position aperture plate against pressure applied by the platen. Screws have been provided to permit minute adjustments of the aperture-plate position in both the vertical and horizontal planes.

#### 6. Planar Lens Mounting

A mounting was designed for the Zeiss Planar 100-millimeter lens which will possibly be used in place of the Japanese Nikkor 150-millimeter lens. The change in focal length of the lens and utilization of the self-contained shutter necessitated changing the entire lens mounting, with the exception of the basic cross slides. The new mounting includes a dial-indicator reading in 0.0005-inch increments. The gage linkage, with a few modifications, is basically the same as that used on Camera I. It is linked to the lens mounting in such a way as to give a precise indication of the lens adjustment along its optical axis.

The design has been left in sketch form without any parts being made, pending the final lens choice.

#### 7. Sensor Head Vacuum Problems

Vacuum tests over the past few weeks have disclosed a very minute air leak in the camera housing. The leak has finally been located in a weld in the area of the magnetic coupler. Intermittent self-sealing has made its identification difficult. The housing has been returned to the vendor to have the weld repaired. There is a possibility that the housing will warp when the heat is applied, but this risk must be taken if the problem is to be overcome.

### B. HIGH-RESOLUTION MONITOR

#### 1. Mechanical Assembly

A basic design for a high-resolution monitor to reproduce the readout signal from the Photo-Tape camera on photographic film, has been formulated. The design, as shown in Figure 19, utilizes an "H"-beam and pedestal construction for

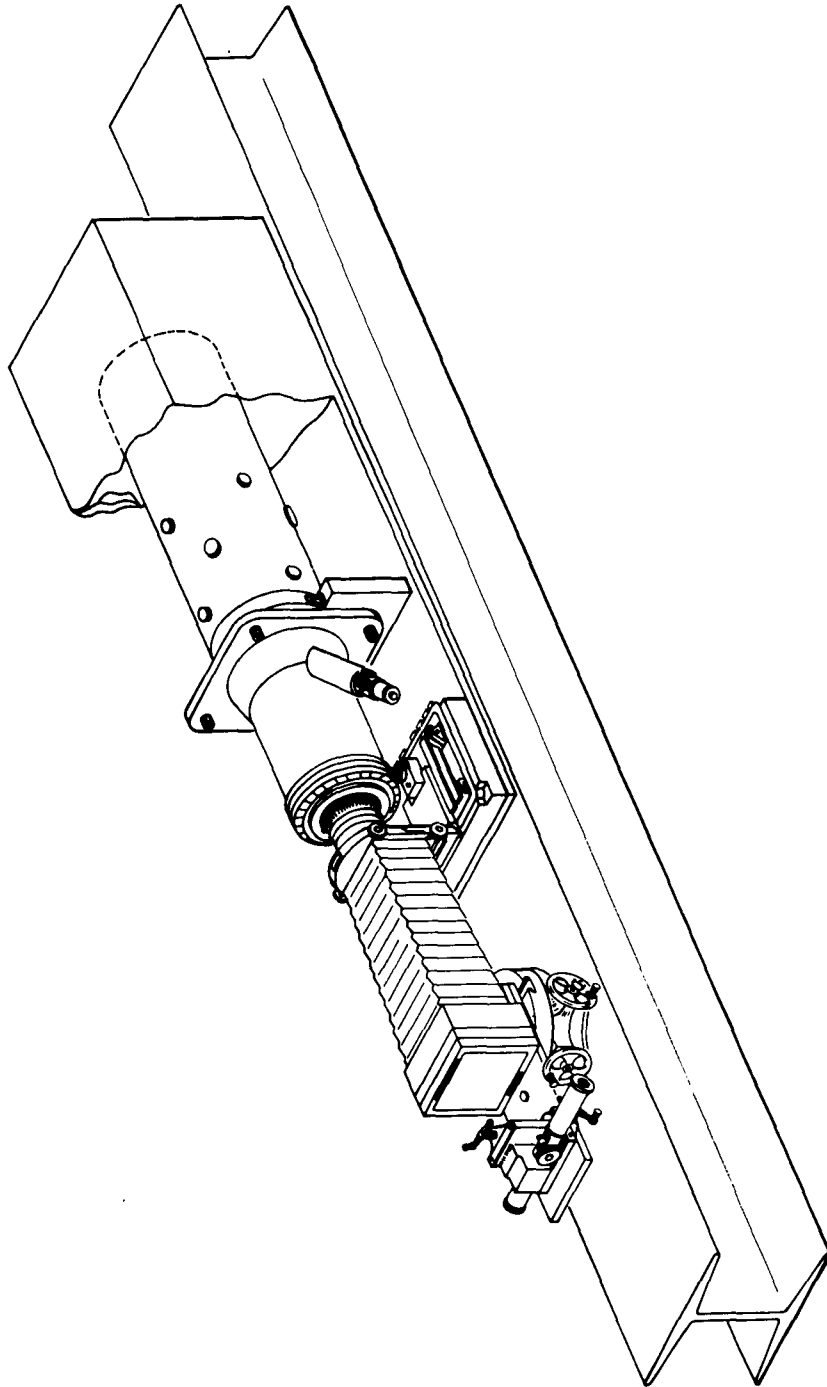


Figure 19. High-Resolution Monitor

the base similar to that employed for Camera II. The cathode-ray tube and its yoke assembly are mounted on one end of the bench with space provided for mounting the associated circuitry. The image from the tube face will pass through a pair of lenses, mounted face-to-face, to the photographic film which will be housed in a Linhof camera. One lens is adjustable for focusing, and its travel along the optical axis can be measured directly on a precision dial indicator.

The Linhof camera housing will be mounted on a common base with a microscope. The latter will be used to look through the assembly to aid in the focusing operation. Cross slides will be used for precision adjustment of the film holder and microscope.

The project is progressing and many of the principal items are already available for integration.

## 2. Circuitry

### a. Video-Amplifier Circuit

The video amplifier for the high-resolution monitor is basically the same as that used on the electron-beam film recorder. It has been fabricated and bench checked. Normal video grid drive voltage for the Dumont cathode-ray tube is ten volts, and it is estimated that "worst-case" drive requirements when overscanning will not exceed 50 volts. The video amplifier has sufficient dynamic range to drive 80 volts peak-to-peak at reduced bandwidth, but will provide 50 volts from d-c to ten megacycles. The output is directly coupled to the grid of the cathode-ray tube and the sync tip is clamped to +30 volts d-c. Both biasing and blanking are accomplished at the cathode.

### b. Horizontal-Deflection Circuit

The horizontal-deflection circuit is the same as that used on Camera II with the exception that the output transformer ratio is 2 to 1 rather than 5 to 1. The 1-millihenry monitor yoke is low impedance, and the flyback voltage developed is not as much as that which occurs in the camera yoke. Normal scanning is accomplished with two amperes peak-to-peak sawtooth current in the monitor yoke while the circuit is capable of delivering nearly ten amperes, or approximately 5 times the normal three-inch frame width. The circuit has been completed and checked and will be mounted in an assembly rack, which will be located beneath the monitor optical bench.

### c. Vertical-Deflection Circuit

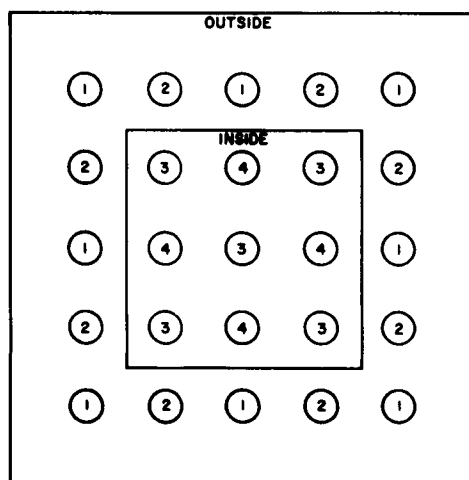
In order to overscan the monitor in the vertical direction, which requires the same magnitude of current as the horizontal winding, due to equal-impedance windings, the output stage has been mounted on an air-cooled heat sink and the feedback resistance has been lowered to 0.5 ohm.



Individual potentiometers have been added for frequency, centering, and amplitude control, respectively, for each of the three possible frame rates. A switching arrangement similar to that used on Camera II selects the charging capacitance, retrace capacitance, and the proper input sync pulse for the desired 6, 1/6, or 1/12 frames-per-second rate. The circuit is otherwise the same as that designed for Cameras I and II, and will deliver nearly ten amperes of current directly coupled to the yoke. The blower output cools the circuitry through a 2.5-inch flexible hose to avoid 60-cycle interference. Bench testing has been completed and integration with all other monitor circuitry has begun.

### C. TEST CHART ILLUMINATOR

The original test chart illuminator was found to be deficient in light output and has been replaced with a larger unit. The new illuminator, as shown in Figure 20 has 25 lamps and combination switches to provide varied patterns of light distribution as well as a wide selection of wattages. Eight light combinations are available. Excess heat is dissipated by means of a blower and a translucent water jacket.



#### LAMP COMBINATIONS

- |                             |                            |
|-----------------------------|----------------------------|
| A-ALL LAMPS 1,2,3 AND 4     | E-INSIDE LAMPS 3 AND 4     |
| B-ALTERNATE LAMPS 1 AND 3   | F-ALTERNATE INSIDE LAMPS 3 |
| C-OUTSIDE LAMPS 1 AND 2     | G-C AND F                  |
| D-ALTERNATE OUTSIDE LAMPS 1 | H-D AND E                  |

Figure 20. Test Chart Illuminator

## SECTION IV. OPTICS

Progress on the camera lens during this reporting period has consisted primarily of clarifying the problems involved, assessing their magnitude, and determining the degree to which they can be solved within the limitations of existing hardware. The results of the Level-B analysis have supplied estimates of performance requirements for the camera objective, and it can be stated with certainty that these requirements will not be met by objectives of the type (commercially available camera lens) thus far used with the camera.

The resolution requirement resulting from the Level-B analysis indicates that the image should display a sine-wave response of at least 80 percent at 85 cycles per millimeter over the 2 1/4 x 2 1/4 inch format of the picture. Additional requirements on the lens are that its f-number be low enough to permit reasonable exposure times, that the image distance be of the order of two inches, and that the lens operate with a vacuum window between it and the image plane.

The problems involved in obtaining an adequate lens stem primarily from the severity of the resolution requirement. The difficulties occasioned by the remaining requirements arise because of the effects that these requirements may have on resolution.

The requirement that the f-number be low enough to permit reasonable exposure periods imposes no additional difficulty, since a lens speed which produces adequate resolution is apparently more than adequate to satisfy the exposure requirements.

The requirement for two-inch clearance on the image side of the lens may be a handicap for two reasons: The first is that this requirement eliminates most, if not all, catadioptric objectives from consideration, since in such objectives the image plane is normally located very close to the primary mirror. This is unfortunate because use of a catadioptric design is the best method of obtaining good color correction in the relatively long focal-length objectives which are desirable for adequately covering the required field. The clearance requirement will also be a handicap in the event that, in recognition of the difficulty of covering the 2 1/4 x 2 1/4 inch format with the required resolution, the format size requirement is relaxed. If this happens, the clearance requirement would prohibit the use of short focal-length objectives which might reasonably be used to achieve the required resolution over a 5- to 10-millimeter circle.

The difficulties arising from insertion of a vacuum window on the image side of the objective cannot be easily assessed. If optimum performance is to be achieved under this condition, the objective should be designed to be used with such a window. However, in the event that a window is used with an objective not specifically designed for its inclusion, the effect of the plate cannot be assessed independently, since the aberrations introduced by the window combine with those of the objective to produce an effect dependent on the aberrations of the particular objective used. Likewise, it cannot be assumed that, if the window does not affect limiting resolution, it will not affect response at 85 cycles per millimeter, since aberrations must cause the greatest loss of response at spatial frequencies intermediate between zero and the limiting frequency.

As noted previously, the principal problem with the lens is meeting the resolution specification. The severity of this requirement can be better understood if the requirement is stated in more familiar terms.

Lens resolution can be studied with reference to the performance of a perfect (aberration-free) lens. The sine-wave response curve for a perfect lens is well documented, and it represents a theoretical upper-limit response for practical systems. The high response called for by the present resolution requirement occurs only towards the lower end of the frequency range for a given lens, and response of a perfect lens in the low-frequency region is approximately linear. The (negative) slope of this straight-line intersects the spatial frequency axis at the point where spatial frequency in cycles per millimeter is equal to  $\pi/4 \lambda F$ , where  $\lambda$  is wavelength in millimeters and  $F$  is the objective f-number. For example, if  $\lambda = 5.5 \times 10^{-4}$  millimeters (the peak of the luminosity curve) and  $F = 5$ , the linear low-frequency approximation of sine-wave response becomes zero at 285 cycles per millimeter. For this example, 80 percent response occurs at 57 cycles per millimeter. Since the Level-B analysis calls for 80 percent response at 85 cycles per millimeter, the specification would be met on axis by a perfect lens having  $F = 3.4$ . (Theoretical response for a perfect lens decreases with increasing field angle; so the f-number would have to be somewhat lower in order to achieve desired resolution over the whole  $2 \frac{1}{4} \times 2 \frac{1}{4}$  inch format.)

There are two distinct problems involved in obtaining a lens of the required quality: first, the problem of locating such a lens since fulfillment of the stated requirement infers the ultimate in lens design; and second, the problem of determining that a particular lens does meet the requirement since techniques for measurement of sine-wave response are as yet not firmly established. With respect to the first problem, many possibilities have been checked, and the only design so far uncovered which comes close to meeting the specifications is a 12-inch focal length,  $f/2$ , lens designed by Perkin-Elmer. Calculated response for this lens is at least 80 percent at 85 cycles per millimeter over a 2-inch diameter circle, but this response is achieved only for light at the sodium D-line ( $\lambda = 589$  millimicrons) and response is substantially worse at other wavelengths. Measured response data for this design is apparently not available. A request has been made for budgeting estimates of price and delivery.

Likewise, with respect to the second problem (measurement of sine-wave response) many possibilities have been checked, and a satisfactory answer is not yet at hand. Measurements have been made previously, but consistent reporting of measured response in excess of perfect lens response leaves some doubt as to the accuracy of this data. Visual and photographic observations of limiting response frequency have been made, but analysis of these results has not been completed. Equipment for sine-wave response measurements has been obtained on loan from Bell Laboratories, but this equipment is not yet in operation.

Work will continue in the two principal problem areas: that of obtaining the lens which most nearly meets the stated specifications, and that of accurately determining the resolution obtained from the chosen lens. In view of the low probability of meeting all the stated requirements within an acceptable time, the search for a lens will take into account the possibility of using a lens which gives the required resolution over smaller formats.

## SECTION V. ELECTRON BEAM FILM RECORDER SUPPORT

A detailed analysis of the EBFR changes, necessary to meet the Level-B requirements, was made at the start of this report period. Since only a few of the areas requiring improvements were provided for in the contract, only limited performance will be obtained. Areas in which work has been started are described in the following paragraphs.

### A. ELECTRON GUN

The present electron gun was operated for 140 hours before the filament burned out. This gun utilizes a special tungsten filament developed at the RCA Laboratories. The spot size was measured to be approximately 1 mil with a beam current of 110 nanoamperes and a grid drive of 20 volts peak-to-peak resulting in a density of 1.1 on Kodak 649 Spectroscopic film, as shown in Figure 21.

A new gun was designed and is being fabricated. Modifications were made in the control grid,  $G_1$ , and  $G_1$ - $G_2$  area to improve the current density in the beam. The filament will be the same as that used in the previous gun. An improved filament design is being fabricated at the RCA Laboratories, and this will be used, as soon as it is available, for the follow-up gun.

### B. DEFLECTION YOKE

The yoke on the EBFR was designed for color TV, and consequently has unequal impedance in the axes. Because of this, different amplifiers are needed in the horizontal and vertical axes, and the deflection axes cannot be interchanged easily for focusing and measuring purposes.

A yoke having equal impedance and resistance in each set of coils was temporarily available and was installed on the recorder to obtain deflection data prior to ordering a new yoke. The sawtooth generators and amplifiers were modified to drive the new yoke, and two sets of pictures were obtained before the gun filament burned out.

Analysis of the pictures showed less beam defocusing with scan. Further details are given in the paragraph on Measurements which appears later in this Report.

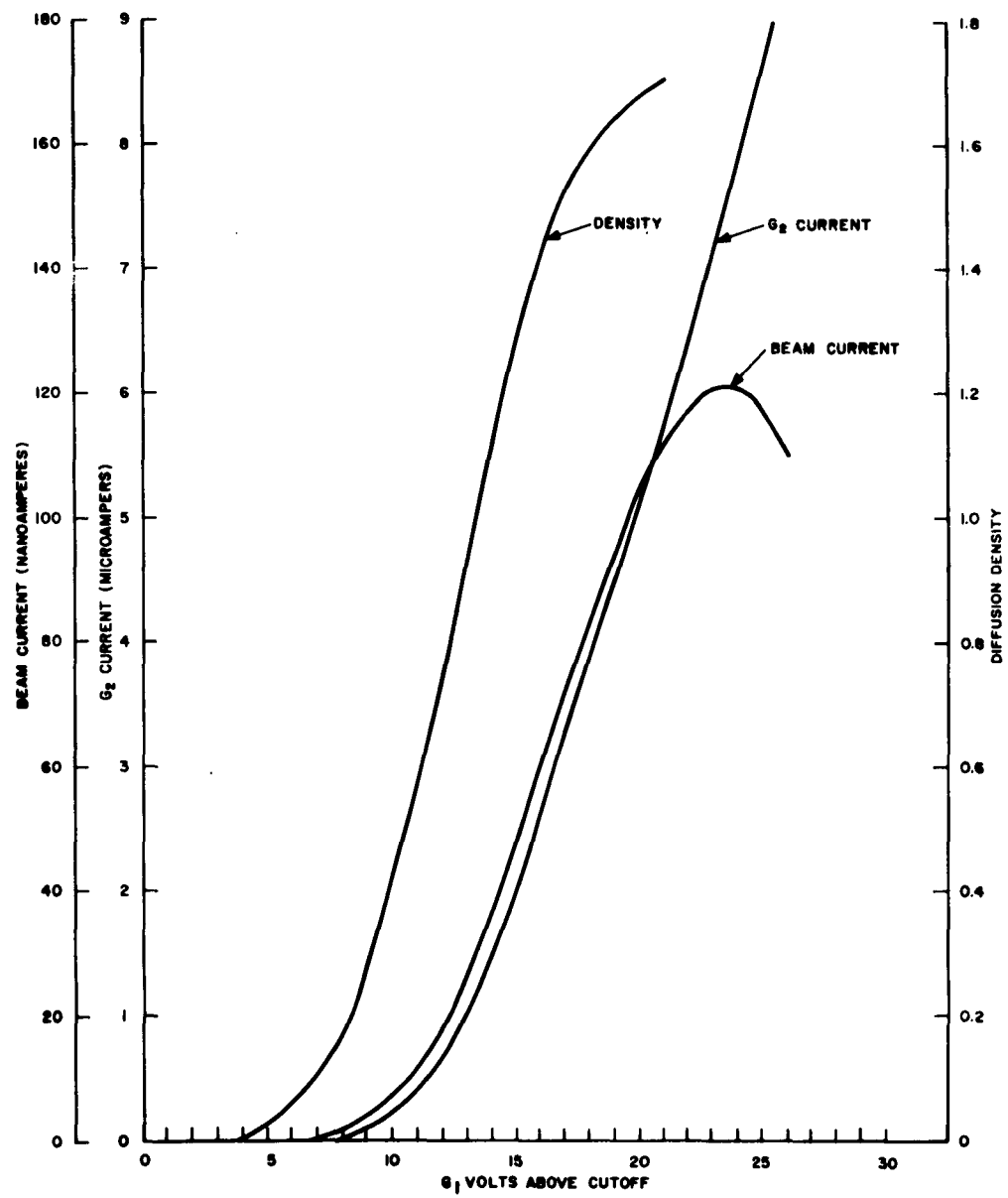


Figure 21. Transfer and Density Characteristics Curves for EBFR Gun No. 4

### C. DYNAMIC FOCUS, CURRENT GENERATOR, AND AMPLIFIER

When an electron beam scans a flat surface the length per unit angle is greater at the center than at the edge. For a  $25^\circ$  scan angle and a 10-inch deflection on axis, the deflection increases 0.25 inch on the horizontal or vertical axis at the picture edge. This means less focus current is required at the edge of the scanned surface than in center. A current generator was borrowed to provide dynamic focus current for the EBFR. This unit has limited capability in that only triangular wave forms with poor stability can be obtained. Because of this limitation, dynamic focus can only be approximated in the outer one-third portion of the picture on axis. Measurements taken with and without dynamic focus show a 2 to 1 reduction in spot size growth.

An investigation is being made to find the best method for generating the proper current wave-shape for dynamic focus. An amplifier will be obtained to drive the dynamic coil when the current generator output is known.

### D. BEAM ALIGNMENT AND SHIELDING

The shield used on the EBFR does not contain any provisions for individual adjustment of the deflection yoke and focus coil. Consequently only a compromise alignment can be obtained, the result of which is a slight displacement of the undeflected spot position as focusing current is adjusted. This means that there is also a displacement of the beam with dynamic focus. A special shield for the high-resolution monitor tube is being checked to see if this design has enough flexibility to use on the EBFR.

An alignment coil has been used to center the beam on the  $G_2$  trimming aperture. This has worked satisfactorily.

### E. FILM AND DEGASSING

All pictures made on the EBFR have been on Kodak 649 Spectroscopic film. This material is supplied on a cellulose triacetate base which has a coefficient of expansion of 0.0035 per  $^\circ\text{F}$  and 0.0077 per 1-percent relative-humidity change. It has recently been learned that this emulsion can be obtained on Estar polyester base and a quantity of this material has been ordered. The polyester base has less than one-half of the coefficient of expansion of triacetate, and in addition it does not have the moisture content. This second feature should be a great advantage in reducing the long degassing time (about 24 hours) now required before the EBFR can be operated after loading with film.

### F. MEASUREMENTS

Spot size is usually measured at the one-half amplitude point. To obtain accurate and consistent readings a recording microdensitometer is required. Measurements of the EBFR spot size have been made on a Jarell-Ash microdensitometer with values

between 0.7 and 1.2 mils obtained. These readings are not reproducible due to the variation in scanning speed of the film holder and the lack of a feedback device to show or compensate for the variation. A Joyce-Loebl microdensitometer was tested and provided completely reproducible results by virtue of the direct connection between the film table and the recording table. The machine available for tests had only a 150-to-1 ratio between tables which did not provide sufficient magnification of the gaussian curve. Ratio arms are available as high as 2000-to-1, which will give more than adequate resolution for future EBFR spots. Since all measurements of density and resolution depend upon a microdensitometer, unless a machine of the Joyce-Loebl type is obtained only estimates of the recorder results can be made.

To obtain individual spots on film a pulse generator capable of 50 to 200 nanosecond wide pulses is required. No such unit is available at present and an astigmatic spot cannot be detected. The only method to obtain best focus is to scan across wires in the film plane and adjust the focus current for the fastest rise time. This method is limited in that a high-gain amplifier and scope is required. Both a Dumont Type 767H and a Hewlett-Packard Type 175 have been borrowed from the vendors and found to be satisfactory. The high-gain Tektronix amplifiers have very limited bandwidth, thereby, rounding off the pulses.

#### **G. BEARINGS**

The unlubricated ball bearings used in the EBFR film reels have frequently caused delays because of binding as a result of operating for many hours in a high vacuum. Bushings made from a Teflon-based material, known as "Chemlon" are being tested as a possible substitute for the ball bearings; however, the latter are preferred because of the free-running characteristic.

The Split Ball Bearing Division of Miniature Precision Bearings Co., Inc., has been identified as the manufacturer and is being solicited to supply new bearings made with "Duroid" ball cages (a teflon-filled material used in the Barden Bartemp bearings). The Bartemp bearings have undergone successful vacuum tests in the RCA Laboratories and are considered satisfactory for use in a vacuum.



CONTRACT AF33(657)-11485  
 DISTRIBUTION LIST (GOVERNMENT)  
 WRIGHT-PATTERSON AFB

No. of Copies		No. of Copies	
	WRIGHT-PATTERSON AFB, OHIO		OTHER DEPT. OF DEFENSE ACTIVITIES
1	ASD (ASNQD) Wright-Patterson AFB, Ohio	1	Hq USAF (AF-RDR) Washington 25, D. C.
1	ASD (AVTE) Wright-Patterson AFB, Ohio	1	Hq AFSC (SCCPR) Attn: Capt. Mauderer Washington 25, D. C.
1	ASD (ASNVEC) Wright-Patterson AFB, Ohio	1	SSD (SAFSP, Attn: Capt. McElhaney) AF Unit Post Office Los Angeles 45, California
1	ASD (AVNT) Wright-Patterson AFB, Ohio	1	Chief, Bureau of Naval Weapons Attn: FFRD-11 Washington 25, D. C.
1	ASD (ASWQS) Wright-Patterson AFB, Ohio	1	RADC (Intelligence Laboratory) Attn: Mr. D. Pantino Griffiss AFB, New York
3	ASD (AVRO) Wright-Patterson AFB, Ohio	1	U. S. Army Signal Research and Development Laboratory Fort Monmouth, New Jersey
1	BWFRR-CD (Attn: Electronics Division) Wright-Patterson AFB, Ohio	1	Director GIMRADA Attn: Librarian Ft. Belvoir, Virginia
1	FTD (TD-D4) Wright-Patterson AFB, Ohio	2	Advisory Group on Electron Tubes 346 Broadway, 8th Floor Attn: Sec. Working Grp on Special Tubes New York 13, New York
	OTHER U. S. GOVERNMENT AGENCIES	1	AFCRL (Electronic Res Library) L. G. Hanscom Fld Bedford, Mass.
1	NASA (GSFC) Code 653 Greenbelt, Md.	1	Air University Library United States Air Force Maxwell AFB, Alabama
1	Advanced Research Projects Agency Attn: ARPD/IDA Technical Library Washington 25, D. C.		
1	DDC Cameron Station Arlington 12, Virginia		

**DISTRIBUTION LIST (GOVERNMENT) (Continued)**

No. of Copies		No. of Copies	
	NON-GOVERNMENT ORGANIZATIONS		NON-GOVERNMENT ORGANIZATIONS (cont.)
1	RAND Corporation Attn: Librarian 1700 Main Street Santa Monica, California	1	CBS Laboratories Attn: B. Linden High Ridge Rd. Stamford, Conn.
1	JPL Attn: Librarian 4800 Oak Grove Pasadena California	1	General Electric Company Attn: W. Chynoweth Rm 251 Bldg 3 Electronics Park Syracuse, New York
1	Aerospace Corporation Attn: Librarian P.O. Box 95081 Los Angeles 45, California	1	Westinghouse Electric Company Attn: A. Jensen, Electronics Lab. Air Arm Division Baltimore, Maryland
1	Aerospace Corporation Attn: Special Projects Office P.O. Box 95081 Los Angeles 45, California		